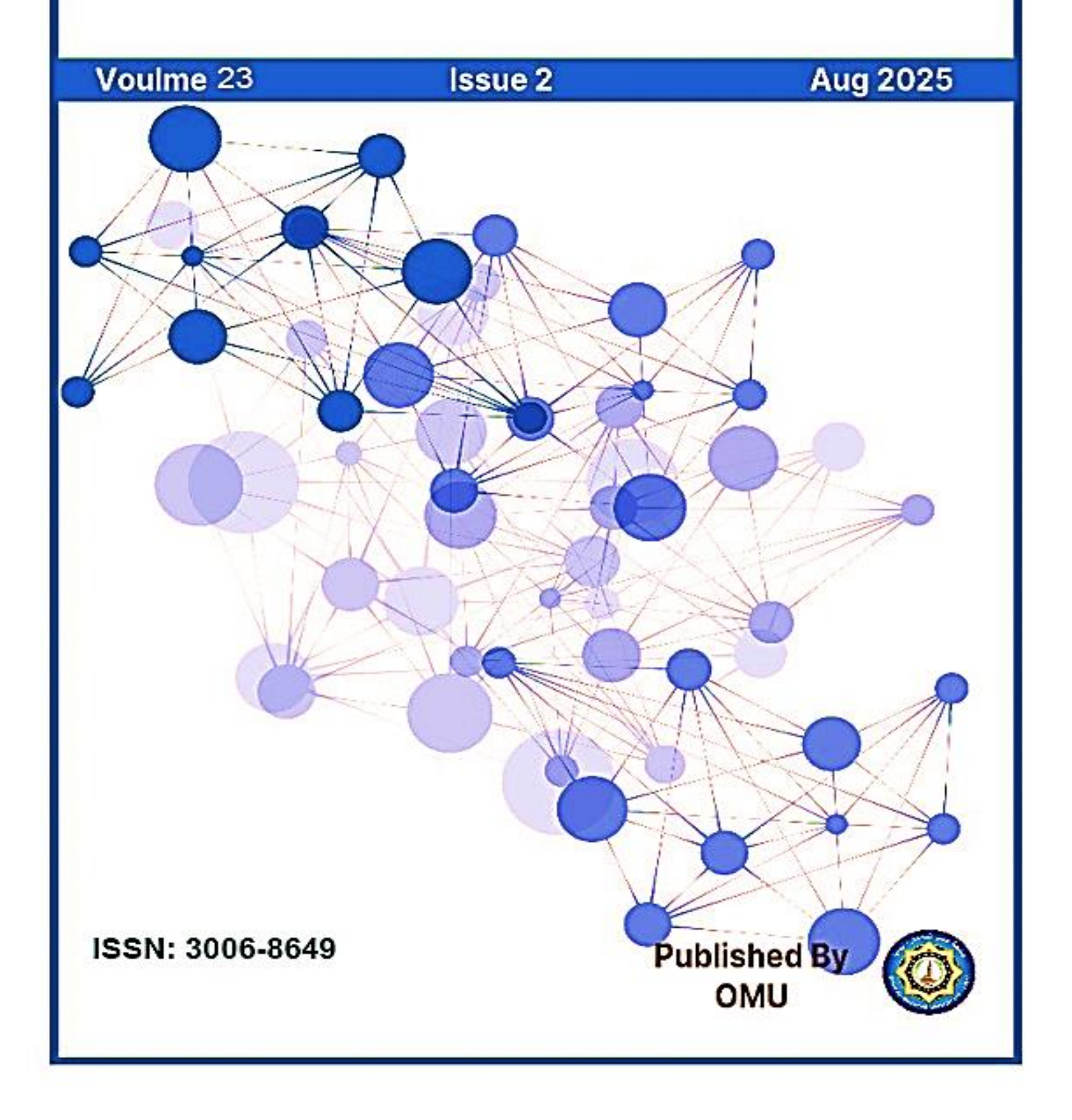
Al-Mukhtar Journal of Basic Sciences



Al-Mukhtar Journal of Basic Sciences

Peer-reviewed scientific journal, Volume Twenty- Three, Issue Tow, 2025

Published by Omar Al-Mukhtar University, Al-Bayda, Libya

The Author(s) 2024. This article is distributed under the terms of the *Creative Commons Attribution-NonCommercial 4.0 International License* (http://creativecommons.org/licenses/by-nc/4.0/), which permits unrestricted use, distribution, and reproduction in any medium, *for non-commercial purposes only*, provided you give appropriate credit to the original author(s) and the source, provide a link to the Creative Commons license, and indicate if changes were made.

A peer-reviewed journal published by Omar Al-Mukhtar University, Al Bayda, Libya

Peer-reviewed scientific journal, Volume Twenty- Three, Issue Tow, 2025

Email: omu.j.bas@omu.edu.ly

EDITORS & STAFF

Prof. Sabah Hassan Lamloum

Editor-in-Chief

Dr.. Mona Muhammad Al-Jabali

Dr.. Jalal Muhammad Abdel Qader

Dr.. Rabha Mohamed Abdel Sayed

Dr., Haifa Muhammad Dozan

Dr.. Salima Saleh Abu Azoum

Dr.. Muhammad Amrja' Muhammad

Dr.. Ruqaya Mahmoud Rashid

Dr.. Essam Abdel Samad

Dr., Rabei Abdul Karim Al-Awami

Heba Juma Abdel Salam, English language auditor

Advisory Board:

Prof.. Hussein Muhammad Al-Barasi, University of Benghazi

Prof. Nouri Hussein Salem Badi, University of Benghazi

Prof.. Ghazi Salama Khammash, Al-Quds University / Gaza

Prof. Hoda Masoud Muhammad, University of Mosul/Iraq

Prof.. Muhammad Al-Hadi Makhlouf, University of Tripoli

Prof.. Iyad Fadel Al-Qayyim Al-Tami, University of Babylon / Iraq

Prof.. Ghalia Thabet Al-Rubaie, University of Benghazi

Prof.. Nidaa Abdul Mohsen Abbas, University of Babylon, Iraq

Prof.. Sufyan Taya, Islamic University/Gaza

Prof... Zaki Abdul Rahman Al-Mustafa for Saudi Arabia / Gaza

Prof.. Khaled Salem Al-Tayeb, University of Tripoli

Prof... Muhammad Ahmed Hamouda, Misrata University

Prof.. Salem Abdel-Aali Al-Shatshat, University of Benghazi

Prof.. Abdul Salam Maatouq, University of Benghazi

Prof. Amjad Abdel Hadi Muhammad, University of Mosul/Iraq)

Prof. Laila Omran Al-Majdoub, Misrata University

Prof. Ali Salem Al-Kharm, University of Benghazi

Al-Mukhtar Journal of Basic Sciences 23: (2), 2025

Papers			Pages
Guanidine as A S	tarting Material for Prepa	ring a Scale Inhibitor	
Othman O. Dakhil	Khaled A. Saleh Mahjoub A. M. Elaoud	Abdulqader A. Imrage	43-59
Assessment of I	Radiation Hazards Parame	ters Associated with	
Natural Radio	onuclides in Granite Used i	n Al-Bayda, Libya	60-67
Jemila M. Ali	Salah S. Basil	Rabea A. Ammar	00 07
Determination of	lead Element in Hair Dye	Samples Available in	
Libyan Mar	kets Using Atomic Absorpt	ion Spectroscopy	
Elham Alterhoni Amina Mohamed Amimn Aya Al-Hadi	· ·	Rabia Omar Eshkourfu f Ebtihal Mustafa Al-Zurqani Afaf Ali Al-Rutbi	68-73
Some Types of r	near Normality Based on So	oft Simply Open Sets	
	Rukaia M. Rashed		74-86
Antioxidant Role of	Cleome Droserifolia Extract	on Cyhalothrin-Induced	
Ox	idative Stress in Male Albi	no Rats	87-95
Nura I. Al-Zail	Salah F. Kamies Salleemah S. Alweeghah	Yasmeen A. Hamad	2. /2

Doi: https://doi.org/10.54172/ej6xtg21

Research Article ⁶Open Access

Guanidine as A Starting Material for Preparing a Scale Inhibitor



Othman O. Dakhil¹, Khaled A. Saleh², Abdulqader A. Imrage³, Mahjoub A. M. Elaoud⁴

- ² Department, of Chemistry, The Libyan Academy of Higher Education, Benghazi, Libya.
- ³ Department of Chemistry, Faculty of Science, University of Benghazi, Benghazi, Libya.
- ⁴ Jowfe Oil Technology, Benghazi, Libya
- *Corresponding author: E-mail addresses: othman-dakeel@gmail.com. Department of chemical pharmacy, Faculty of Pharmacy University of Benghazi Benghazi-Libya

Received:

16 February 2025

Accepted:

28 August 2025

Publish online:

31 August 2025

Abstract

This study presents the synthesis and evaluation of a novel phosphonatebased scale inhibitor using guanidine as the starting material. Given guanidine's highly reactive nature and multiple substitution sites, it was chemically modified by introducing phosphonomethyl groups to enhance its scale inhibition capabilities. The synthesized compound was structurally characterized using FT-IR, ¹H NMR, ¹³C NMR, and mass spectrometry, confirming successful substitution of three hydrogen atoms with phosphonate groups. The compound's performance was assessed through static scale inhibition tests at various temperatures (40°C, 60°C, and 70°C) for calcium carbonate and calcium sulfate, showing significant inhibition at concentrations as low as 20–30 ppm. Titration-based calcium analysis revealed inhibition efficiencies up to 100%. Additionally, the compound demonstrated good compatibility with calcium and acceptable seawater biodegradability over 28 days. These results suggest that the synthesized inhibitor is a promising candidate for environmentally safer and thermally stable scale control in industrial water systems.

Keywords: Guanidine, Scale Inhibitor, Phosphonate Compound, Chelation, Calcium Carbonate, Calcium Sulfate, Biodegradability.

INTRODUCTION

Oilfield scaling is a widespread challenge in the oil and gas sector, leading to substantial financial losses due to property damage and decreased production. This issue, ranking among the top production efficiency impediments, is pervasive worldwide, primarily affecting water-related oil extraction operations alongside corrosion and hydrate formation. Scaling can accumulate on various surfaces, particularly around the wellbore, restricting fluid flow and obstructing production equipment from pore throats to processing facilities. The industry typically encounters four major types of scale: Calcium Carbonate (calcite and aragonite), Calcium Sulfate Salts (like gypsum), Strontium Sulfate (celestite), and Barium Sulfate (barite).

Scale inhibitors (SIs) are the primary solution used to prevent crystal growth and scale formation, with concentrations ranging from 1 to 500 ppm to maintain effectiveness. Water-soluble organic SIs are most common in the industry, where it is critical to sustain concentration above the minimum



The Author(s) 2025. This article is distributed under the terms of the *Creative Commons Attribution-NonCommercial 4.0 International License* ([http://creativecommons.org/licenses/by-nc/4.0/] (http://creativecommons.org/licenses/by-nc/4.0/]), which permits unrestricted use, distribution, and reproduction in any medium, *for non-commercial purposes only*, provided you give appropriate credit to the original author(s) and the source, provide a link to the Creative Commons license, and indicate if changes were made.

inhibitor concentration (MIC) to ensure efficacy. SIs are commonly applied through downhole squeeze treatments or continuous injection at the wellhead (Kelland, 2014). In squeeze treatments, inhibitors are injected into the subsurface formation, often using seawater to extend their reach, after which the inhibitors are absorbed by the formation rock near the wellbore and released gradually into the produced water, effectively controlling scale during production. Phosphoric acids, particularly those with C-PO(OH)2 moieties, are an important class of organophosphorus compounds (Garber et al., 2016; Kiran et al., 2008).

These compounds and their derivatives, known as phosphates, are widely used across agricultural, chemical, and pharmaceutical industries (Ash, 2004; Kukhar & Hudson, 2000). Organophosphonic acids and their salts are essential scale inhibitors in the oil industry (Demadis, 2006; Jordan & Mackay, 2007; Woodward et al., 2004). These inhibitors vary in structure, from small non-polymeric molecules with limited phosphonate groups to more complex polymeric compounds with a higher phosphonate concentration (Kelland, 2014). In many cases, phosphonate groups are bonded to aminomethylenephosphonate structures, where the amine acts as a Lewis base ligand, further enhancing scale inhibition.

Phosphonate groups in scale inhibitors serve a functional role in indicating inhibitor concentration in produced water. Their presence aids in determining the timing for re-squeeze operations to ensure continuous scale inhibition. Phosphonate groups are especially advantageous in the oilfield industry for mitigating scale issues due to their durability and biodegradability.

MATERIALS AND METHODS

Previous studies (Mady & Kelland, 2017) have shown that conjugating amino phosphonates with methylene phosphonates significantly improves the effectiveness of scale inhibitors, though biodegradability remains a challenge, as seen in BP-7 and BP-9, which exhibited low biodegradation rates. This study focuses on synthesizing a new scale inhibitor using guanidine as a starting material. Research suggests that phosphonate groups can effectively replace hydrogen atoms bound to nitrogen in guanidine, enhancing the compound's ability to prevent scaling. Furthermore, the inhibitory efficiency is expected to increase with the number of phosphonate groups attached. Consequently, guanidine, with its five hydrogen atoms, provides a promising molecular framework for this investigation, as shown in Scheme 1.

Scheme (1). ((dihydroxyphosphaneyl)methyl)-1.3.3- tris(phosphonomethyl)guanidino) methyl) phosphonic acid

Guanidine is a hygroscopic organic compound with the chemical formula CH₅N₃ and a molecular weight of approximately 59.07 g/mol. It is a colorless solid that is soluble in polar solvents and possesses strong basic properties. Guanidine is not only found as an independent molecule but also as a constituent in larger organic compounds, including arginine side chains, and occurs naturally in various sources such as urine, turnip juice, mushrooms, rice husks, and muscle tissue. Its melting point

is around 50°C, and upon heating to 160°C, it converts to melamine and ammonia. For the development of an effective and environmentally friendly scale inhibitor, certain criteria must be met (Mady & Kelland, 2017). These include chieving a minimal effective concentration of 1 to 100 ppm, with an optimal range of 1 to 5 ppm; maintaining thermal stability at temperatures up to 100°C and between 130°C to 170°C; exhibiting at least 60% biodegradability within 28 days; having a pH compatibility range of 4 to 9; compatibility with calcium; and being cost-efficient in production and application.

In addition to its potent therapeutic effects, guanidine's molecules belong to an indisputable family of chemicals that are distinguished by their ability to acquire a positive charge through protonation in physiological settings (Kim et al., 2021; Zamperini et al., 2017). Guanidine groups play a crucial role in the development and identification of antibiotics because of this characteristic, which enables them to establish hydrogen bonds or electrostatic interactions with possible bacterial targets (Kim et al., 2021). One common example of this type of chemical is the antibiotic streptomycin, which has a guanidine group (Moussa, 2014). Guanidine-functionalized groups can be added to polycarbonates as an adjuvant, greatly increasing the antibacterial activity of several antibiotics (Zamperini et al., 2017).

Guanidine can be isolated from several of the medications in which it is used; thus, purchasing it is not necessary. By repurposing old medications rather than discarding them, this approach guarantees environmental preservation. The ketophane molecule was extracted from the medicine it contains and reused in chemical reactions in a scientific investigation (Dakhil et al., 2022).

Scale Inhibitors

A scale inhibitor is a chemical agent designed to prevent the formation of scale by reducing the rate of fouling scale development (Delon Jimenez, 2014). These inhibitors typically comprise water-soluble compounds that effectively impede the nucleation and crystal growth of inorganic scales by disrupting normal crystal growth patterns, thereby preventing larger crystal formations. Certain polymers have been identified as effective nucleation inhibitors and dispersants (Kelland, 2014) . Key characteristics of an effective scale inhibitor include:

- Efficiency: It must effectively inhibit scale formation, regardless of the mechanisms involved.
- **Stability:** The inhibitor should remain stable under the elevated temperatures found in oil production environments.
- **Compatibility:** It must not interfere with other oilfield chemicals or change in response to their presence, while integrating smoothly with chemical injection systems.

To ensure comprehensive protection against scale formation, maintaining a minimum inhibitor concentration (MIC) is crucial; concentrations below this threshold significantly increase the risk of scale formation. In the oilfield, common scales like carbonates and sulfates contain divalent anions (CO₃²⁻ and SO₄²⁻) alongside group II metal cations. The scale inhibitor must interact with these anions or cations to anchor effectively to the scale surface and prevent competing molecules from binding to the crystal lattice (Kelland, 2014).

Various organic molecules with anionic groups can interact favorably with group II cations on scale crystal surfaces. The most prevalent anionic groups include phosphates, phosphonates, phosphinates, carboxylates, and sulfonates (Kelland, 2014). Molecules containing multiple anionic groups or mixtures of these have been effective as scale inhibitors, particularly when in their anionic dissociation form. Common classes of scale inhibitors include polyphosphates, phosphates, small

non-polymeric phosphonates and aminophosphonates, polyphosphonates, polycarboxylates, phosphino polymers, and polysulfonates (Kelland, 2014).

Phosphate esters are recognized for being environmentally friendly scale inhibitors, although they may not be the most efficient. Their solubility in water or oil can be adjusted by modifying the alkyl tail length of the alcohol used in their synthesis. Additionally, compact non-polymeric scale inhibitors, characterized by limited phosphonate groups, show effectiveness due to their aminomethylenephosphonate groups, which can form bonds with divalent cations, enhancing the chelation effect and stabilizing complexes (Mady & Kelland, 2017).

Research has highlighted the importance of bisphosphonates (BP), which have been used for decades in treating bone disorders due to their targeting properties (Ebetino et al., 1998; Maeda, 2004; Sparidans et al., 1998). These compounds are resistant analogs of pyrophosphates that inhibit mineralization processes in bones (Hirabayashi et al., 2002; Rodan & Martin, 2000). However, phosphonate-based scale inhibitors often face criticism for their limited biodegradability, which raises environmental concerns as both the water treatment industry and oil companies focus on the implications of these compounds (Popov et al., 2016).

The biodegradability of scale inhibitors is categorized by their environmental impact, with "Green" or "Yellow" classifications indicating a minimum biodegradation rate of 20% within 28 days, according to the Norwegian national environmental agency (Nowack, 2003). Conversely, "Red" category chemicals exhibit less than 20% biodegradation. Presently, environmentally friendly scale inhibitors lack stability at high reservoir temperatures exceeding 140°C. Over-extended periods resulting in a scarcity of effective options for near-wellbore regions. Scale squeeze treatments are utilized to address this issue by injecting inhibitors into formations, where they adhere to reservoir rocks and are gradually released, necessitating thermal stability for long-term effectiveness.

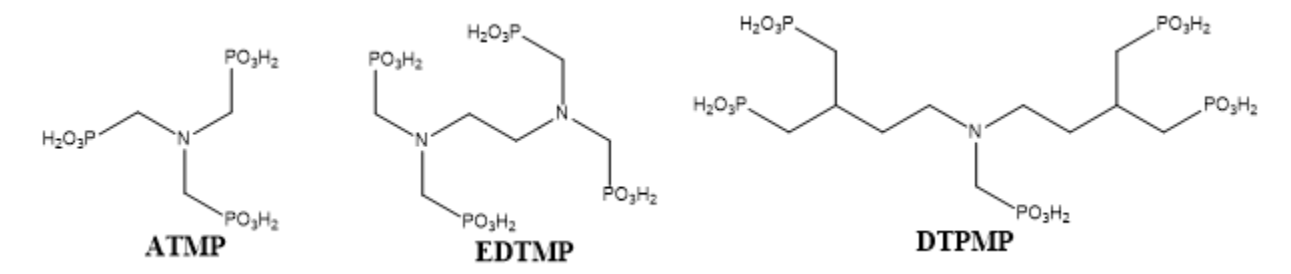


Figure (1). Common oilfield SIs containing Phosphonate Groups (Mady & Kelland, 2017).

Chemicals and Reagents

Guanidine used in the experiments in the experimental comes from India. It is imported and distributed by Chang Chun Chan Enterprise Sdn Bhd Company. Phosphorous acid (H₃PO₂), hydrochloric acid (HCI), and formaldehyde (CH₂O) from Riedel-de Haën Company. It was purchased from Egypt for the University of Benghazi.

The reagents used for performance were Sodium Chloride (NaCl) and Calcium chloride (CaC₁₂.2H₂O) supplied by (Amazon), Sodium sulfate (Na₂SO₄), and sodium Bicarbonate (NaHCO₃) comes from India.

Instrumentation and Apparatus

- A magmatic Stirrer (FAIC instrument laboratory equipment supplier in Italy). and Precision balance 440 43 (Shon GmbH, GERMANY) was utilized as the mathematical instrument in the experiment.
- A Hamilton micro syringe was used in this preliminary study for sampling.
- OEM digital pH measuring device, water quality. A tester was used.
- Used glassware from Witeg Labortechnik GmbH (Germany).
- All previous appliances, tools, and glass were purchased from Modern Science Company, Benghazi.
- ¹H and C¹³ NMR analyses were performed, and spectra were recorded using equipment at the National Research Center Central Laboratory Services Magnetic Resonance Laboratory, Cairo, Egypt.
- Fourier Transform Infrared (FT-IR) spectroscopy was employed to elucidate the molecular structure and functional group composition of the synthesized inhibitor. The analysis was conducted using an Agilent Technologies Cary 630 FT-IR spectrometer at the Libyan Advanced Center for Chemical Analysis in Tajoura, Tripoli.

A JASCO instrument. The samples were scanned with a resolution of 4 cm⁻¹ over a wavenumber range of 550-4000 cm⁻¹ at the National Research Center – Central Laboratory Services – Magnetic Resonance Laboratory, Cairo, Egypt.

Experiments and tests were conducted in the laboratory of the Libyan Academy for Postgraduate Studies in Benghazi within the timeframe specified by the academy, lasting approximately five months. The project began in February 2023, with trial and performance evaluations concluding in July 2023. This phase marks a crucial step in the experiment before transferring it to external laboratories for further analyses, as outlined in this research.

Syntheses of Scale Inhibitor.

As illustrated in the figures (2,3), guanidine (5g, 84.6 mmol) was in a two-neck flask. Phosphorous acid (34.68g, 423 mmol) was added into the flask, while stirring, the HCl (15. 41 g, 423 mmol) was added dropwise into the mixture, and heated in a water bath for 10 min.at 100°C. Formaldehyde (12.7g, 423 mmol) was then added dropwise into the solution while stirring and heating at look. The reaction was then left overnight at 100°C. Then the mixture was filtered, and The Solvent of the liquid Phase was removed under reduced pressure. Scheme 2.

Scheme (2). Phosphonation of Guanidine Diamine with Phosphorous Acid. Formaldehyde and HCl (Rodan & Martin, 2000).

RESULTS AND DISCUSSIONS

Results Scale Test Observations

To summarize the findings from scale tests at various temperatures and concentrations, the following tables provide detailed observations.

Table (1). Scale Test Observations at (40°C) CaCO₃

Product	Dose (ppm)	0 hr.	1 hr.	2 hr.	4 hr.	8 hr.	24 hr.
	0	*C,B	*Sl haze	S1 haze	*S1 CO ₃ ppt	*CO ₃ ppt	*hvy CO ₃ ppt
	5	C,B	C,B	C,B	S1 haze	*S1 CO ₃	*CO ₃ ppt
Dlanla	10	C,B	C,B	C,B	S1 haze	S1 CO ₃	CO ₃ ppt
Plank	15	C,B	C,B	C,B	S1 haze	S1 haze	Sl CO ₃ ppt
	20	C,B	C,B	C,B	S1 haze	S1 haze	Sl CO ₃ ppt
	30	C,B	C,B	C,B	C,B	C,B	S1 haze

Table (2). Scale Test Observations at (40°C) CaSO₄

Product	Dose (ppm)	0 hr.	1hr.	2 hr.	4 hr.	8 hr.	24 hr.
	0	C,B	C,B	C,B	*S1 SO ₄ ppt	*SO ₄ ppt	*hvy SO ₄ ppt
	5	C,B	C,B	C,B	C,B	*S1 SO ₄ ppt	*SO ₄ ppt
DI 1	10	C,B	C,B	C,B	C,B	Sl SO ₄ ppt	SO ₄ ppt
Plank	15	C,B	C,B	C,B	C,B	Sl SO ₄ ppt	SO ₄ ppt
	20	C,B	C,B	C,B	C,B	C,B	Sl haze
	30	C,B	C,B	C,B	С,В	С,В	С,В

Table (3). Scale Test Observations at (60°C) CaCO₃

Product	Dose (ppm)	0 hr.	1hr.	2 hr.	4 hr.	8 hr.	24 hr.
	0	C,B	S1 haze	Sl haze	S1 CO ₃ ppt	CO ₃ ppt	hvy CO ₃ ppt
	5	C,B	C,B	C,B	S1 haze	S1 CO ₃	CO ₃ ppt
DI 1	10	C,B	C,B	C,B	S1 haze	Sl CO ₃	CO ₃ ppt
Plank	15	C,B	C,B	C,B	Sl haze	S1 haze	S1 CO ₃ ppt
	20	C,B	C,B	C,B	Sl haze	S1 haze	S1 CO ₃ ppt
	30	C,B	C,B	C,B	C,B	C,B	S1 haze

Table (4). Scale Test Observations at (60°C) CaSO₄

Product	Dose (ppm)	0 hr.	1hr.	2 hr.	4 hr.	8 hr.	24 hr.
	0	C,B	C,B	C,B	Sl SO ₄ ppt	SO ₄ ppt	hvy SO ₄ ppt
	5	C,B	C,B	C,B	C,B	Sl SO ₄	SO ₄ ppt
D1 1 .	10	C,B	C,B	C,B	С,В	Sl SO ₄	SO ₄ ppt
Plank	15	C,B	C,B	C,B	С,В	Sl SO ₄	SO ₄ ppt
	20	C,B	C,B	C,B	С,В	C,B	Sl haze
	30	C,B	C,B	C,B	C,B	C,B	C,B

Table (5). Scale Test Observations at (70°C) CaCO₃

Product	Dose (ppm)	0 hr.	1hr.	2 hr.	4 hr.	8 hr.	24 hr.
	0	C,B	Sl haze	Sl haze	Sl CO ₃ ppt	CO ₃ ppt	hvy CO ₃ ppt
	5	C,B	C,B	C,B	S1 haze	S1 CO ₃	CO ₃ ppt
Dlaula	10	C,B	C,B	C,B	S1 haze	S1 CO ₃	CO ₃ ppt
Plank	15	C,B	C,B	C,B	S1 haze	Sl haze	Sl CO ₃ ppt
	20	C,B	C,B	C,B	S1 haze	Sl haze	Sl CO ₃ ppt
	30	C,B	C,B	C,B	C,B	C,B	Sl haze

Table (6). Scale Test Observations at (70°C) CaSO₄

Product	Dose (ppm)	0 hr.	1hr.	2 hr.	4 hr.	8 hr.	24 hr.
	0	С,В	C,B	C,B	Sl SO ₄ ppt	SO ₄ ppt	hvy SO ₄ ppt
	5	C,B	C,B	C,B	С,В	Sl SO ₄	SO ₄ ppt
Dlaula	10	C,B	C,B	C,B	С,В	Sl SO ₄	SO ₄ ppt
Plank	15	C,B	C,B	C,B	C,B	Sl SO ₄	SO ₄ ppt
	20	C,B	C,B	C,B	C,B	C,B	Sl haze
	30	C,B	C,B	C,B	C,B	C,B	C,B

Where:

^{*}hvy SO₄ ppt = Heavy Sulfate Precipitate



Figure. (2). Scale Test Observation for CaCO₃ at 70°C

^{*}C&B = Clear and bright

^{*}Sl haze = Slight haze

^{*}Sl CO₃ ppt = Slight Carbonate Precipitate

^{*}CO₃ ppt = Moderate Carbonate Precipitate

^{*}SO₄ ppt = Moderate Sulfate Precipitate

^{*}Sl SO₄ ppt = Slight Sulfate Precipitate

^{*}hvy CO₃ ppt = Heavy Carbonate Precipitate



Figure. (3). Scale Test Observation for CaSO₄ at 70°C

Effect of The Inhibitor on Crystal Modification: Results

The presence of PBTC (Phosphonobutane-1,2,4-Tricarboxylic Acid) in solutions containing CaCO₃ leads to changes in crystal morphology, resulting in rounded corners and the formation of aggregates. However, the number of crystals formed in the presence of PBTC is statistically fewer. Aggregation of CaCO₃ crystals can also be observed with certain additives. FT-IR analysis of PBTC-treated CaCO₃ crystals indicates the presence of bands associated with the -PO₃ group, suggesting inhibitor incorporation within the CaCO₃ lattice or at the crystal edges.

Results of the Titration Technique

The results of the scale test for CaCO₃ are summarized in (Table 7).

Table (7). Scale Test CaCO₃

Product	Dose PPM	Titration Reading	Ca sample mg/L	Ca sample mg/L Ca Blank mg/L	Percentage inhibitor %
	0	3.4	272	0.00	0.00
	5	3.8	304	32	11
Blank	10	4.6	368	96	35
	20	5.8	464	192	70
	30	6.8	544	272	100

The results of the scale test for CaSO₄ are summarized in (Table 8).

Table 8: Scale Test CaSO₄

Product	Dose PPM	Titration Reading	Ca sample mg/L	Ca sample mg/L Ca Blank mg/L	Percentage inhibitor %
	0	4.2	457.2	0.00	0.00
	5	4.8	522.77	65.57	16.3
Blank	10	5.9	642.5	185.3	46
	20	7.1	773.27	316.07	78.4
	30	7.9	860.4	403.2	100

Results of Compatibility with Calcium Test

In (Figure 4) shows the results of the compatibility test with calcium ions, The bottles in the Figure shows the test after 24 hours, all bottles with clear solutions.



Figure.(4). Compactivity test in 100 ppm Ca²⁺ and 3% NaCl in 2 ml.

Results of High-Pressure Dynamic Tube Blockage Test

Table (9). The Composition of Sulphate Brine 1 And Brine 2 Used in The Scale-Rig

Brine 1					
ion	ppm		g/L	g/3L	g/5L
Na	19510	NaCl	38.640	115.93	193.2
Ca	2040	CaCl ₂ * 2H ₂ O	5.3100	15.930	26.55
Mg	530	MgCl ₂ * 6H ₂ O	13.660	40.980	68.30
K	1090	KCl	1.9200	5.7600	9.600
Ba	570	BaCl ₂ * 2H ₂ O	0.5100	1.5300	2.550
Sr	290	SrCl ₂ * 6H ₂ O	0.4400	1.3200	2.200
Cl		Actual Cl ppm	31166.40		
Brine 2					
ion	ppm		g/L	g/3L	g/5L
Na	19510	NaCl	35.04	105.12	175.20
SO_4	2960	Na ₂ SO ₄ Anhydrous	4.380	13.149	21.900
		Actual Cl ppm	30086.4	7	

Table (10). The Composition of Carbonate Brine 1 And Brine 2 Used in The Scale-Rig

Brine 1					
ion	ppm		g/L	g/3L	g/5L
Na	19510	NaCl	49.59	148.77	247.97
Ca	2040	CaCl ₂ * 2H ₂ O	7.48	22.45	37.42
Mg	530	MgCl ₂ * 6H2O	4.43	13.30	22.16
K	1090	KCl	2.0781	6.23	10.39
Ba	570	BaCl ₂ * 2H ₂ O	1.0138	3.04	5.07
Sr	290	SrCl ₂ * 6H ₂ O	0.8824	2.65	4.4122
Cl	0	Actual Cl ppm	35633.19		
Brine 2					
ion	ppm		g/L	g/3L	g/5L
Na	19510	NaCl	49.59	148.77	247.95
SO_4	2000	Na ₂ SO ₄ Anhydrous Actual Cl ppm	2.76	8.26	13.76

Results of Scale Inhibitor Seawater Biodegradability Test

Oxygen consumption data were recorded over a 28-day duration, while all flasks were incubated in darkness at 20°C. At the end of the 28-day period, data were collected, and results were obtained. The ThOD (Theoretical Oxygen Demand) for each scale inhibitor was calculated in accordance with OECD 306 guidelines, accounting for complete nitrification. Background respiration values (BOD values representing seawater's inherent respiration) were subtracted from the BOD of each test compound prior to determining the percentage of biodegradability, as per OECD.

FT-IR SPECTROSCOPY

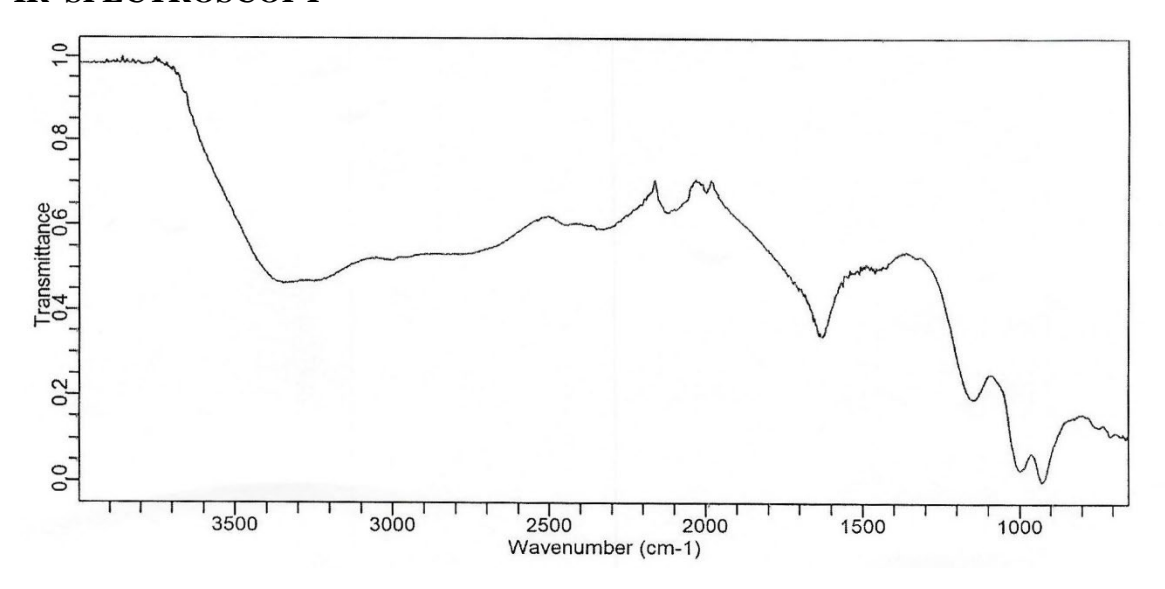


Figure.(5). FTIR Spectra for Guanidine

The spectra clearly show a peak at a wavelength of approximately 3000-3300 nm, which corresponds to the characteristic wavelength of the CH₂-CH group added to guanidine, which does not contain the CH₂ group in its structure.

The presence of a signal at 2117 indicates the presence of a non-exchangeable C=N bond associated with the sp3 nitrogen atom of the NH group, as previously explained. This further supports the facile substitution of hydrogen atoms on the sp3 nitrogen atom compared to the difficulty of substituting hydrogen atoms on the sp3 nitrogen atom in guanidine.

Results of NMR Spectroscopy

Analysis was performed to confirm the formation of the target compound and to elucidate its detailed structure. This involved employing two powerful spectroscopic techniques: Carbon-13 Nuclear Magnetic Resonance C¹³NMR and Proton Nuclear Magnetic Resonance ¹H NMR. These techniques provide complementary information about the molecule. C¹³NMR spectroscopy probes the chemical environment of the carbon atoms within the molecule, revealing the number of carbons and their connectivity. ¹H NMR spectroscopy, on the other hand, focuses on the hydrogen atoms, providing details about their chemical shifts and coupling patterns. By analyzing both C¹³NMR and ¹H NMR spectra, chemists can gain a comprehensive understanding of the target compound's structure, including the presence of functional groups and the arrangement of atoms within the molecule.

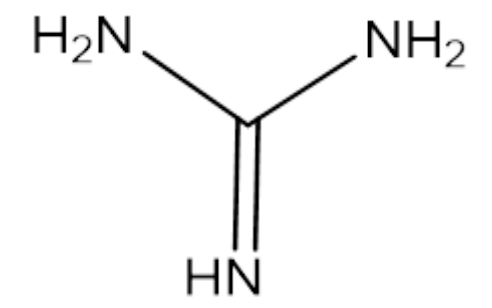


Figure.(6). Structure of Guanidine

The strategic substitution of 5 hydrogen atoms with specific functional groups aims to produce the target compound with tailored electronic properties and enhanced reactivity.

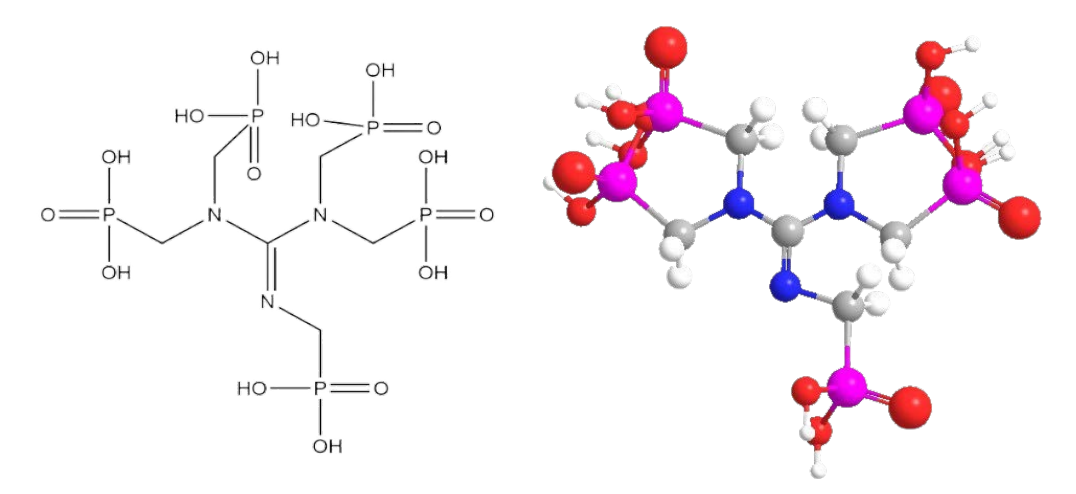


Figure.(7). 2D & 3D – {bis [bis (phosphonomethyl) amino] methylene} phosphoramidic acid

However, analysis revealed incomplete substitution, with only 3 hydrogen atoms replaced by phosphonate groups (H₃PO₃), likely due to the combined effects of strong SP²N bond strength, insufficient reaction time, and steric hindrance in the resulting molecule:

- The substitution of hydrogen on an SP²N atom is difficult due to the strength of the SP²N bond.
- The steric hindrance of the resulting compound prevented the substitution of the fourth hydrogen atom on the SP³ nitrogen atom. The resulting compound is shown in the following structure.

Figure.(8). [(N-methyl – N – (phosphonomethyl) carbamimidyl) azanediyl) bis (methylene) bis (phosphonic acid)]

Results of NMR C¹³ Spectroscopy

C¹³ NMR spectroscopy will be used to analyze the carbon framework of the synthesized molecule. This technique differentiates between various carbon types (methyl, carbonyl, etc.) based on their environment, aiding in confirming the success of the functional group substitution.

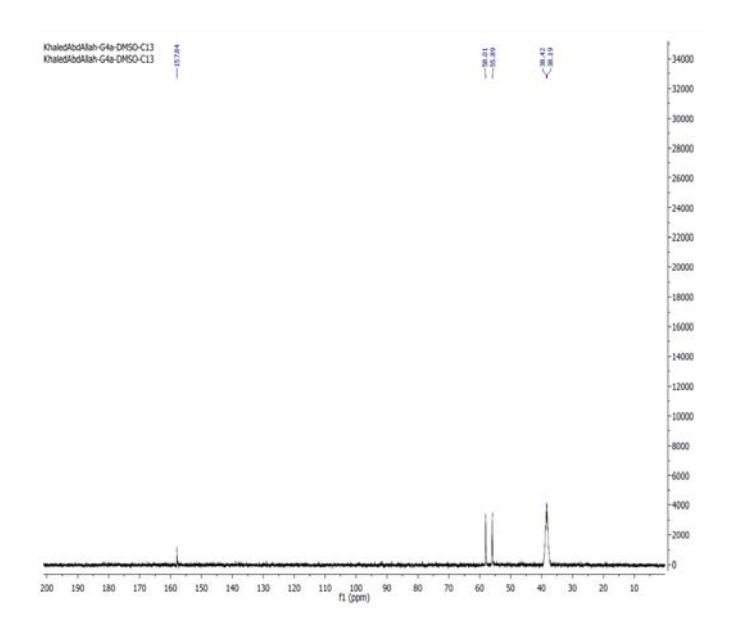


Figure.(9). C13 NMR Spectrum for Guanidine

C-	38.19 ppm	CH3
C-	38.42 ppm	CH3
C-	55.9 ppm	CH2
C-	58.01 ppm	CH2
C-	58.01 ppm	CH2
C-	157.84 ppm	C

Results of ¹H NMR Spectroscopy

¹H NMR spectroscopy will be employed to analyze the chemical environments of hydrogen atoms in the synthesized molecule. This technique aids in confirming the success of functional group substitution by identifying the number and location of hydrogens.

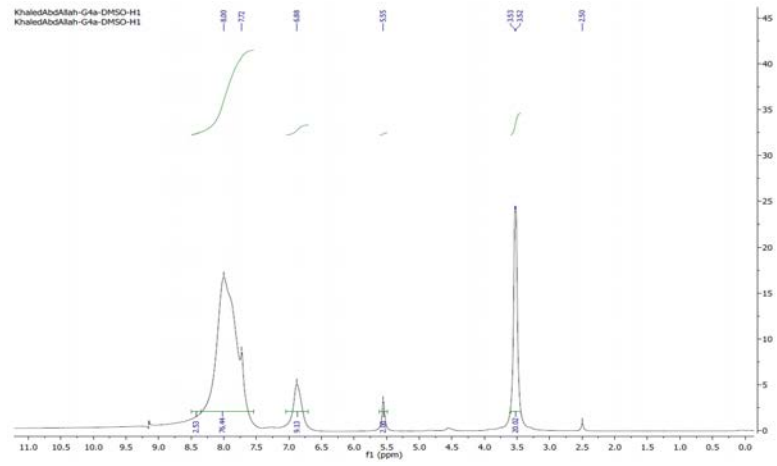


Fig.(10). ¹H NMR Spectroscopy for Guanidine

OH	5.5 ppm
OH	5.5 ppm
NH	7.72 ppm
CH2	3.5 ppm
CH2	3.5 ppm
CH2	3.5 ppm

Results of Mass Spectroscopy (Ms)

The compound underwent fragmentation, producing a Molecular ion peak (M+) at M/2 = 372 with a relative intensity of 171.1 on the spectrum (Figure 11). This peak represents the molecular weight of the compound under study.

The spectrum also showed a Base peak (Beas peak) at M/2 = 81, corresponding to the molecular weight of PO_3H_2 (phosphoric acid monohydrate) with a significant relative intensity of 289506.

A prominent peak at the top of the spectrum with M/2 = 64 and an exceptionally high relative intensity of 639943.1 could be attributed to the Beas peak of PO₂ (phosphorus dioxide).

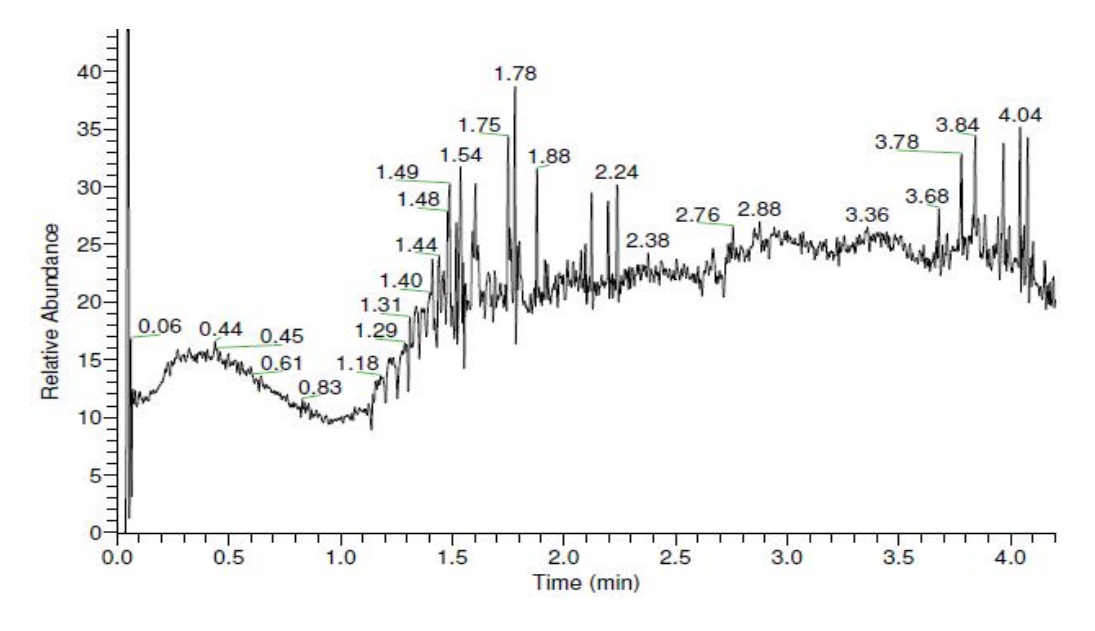


Figure (11). MASS SPECTROSCOPY (MS) spectrum of the compound under study

DISCUSSION

The aim of this study was to synthesize a novel, environmentally conscious scale inhibitor based on guanidine, leveraging its unique molecular structure and reactivity to achieve effective inhibition of common oilfield scales—primarily calcium carbonate (CaCO₃) and calcium sulfate (CaSO₄). The experimental results support the initial hypothesis that functionalizing guanidine with phosphonate groups would yield a compound with significant scale-inhibition capabilities, especially under elevated temperature conditions.

Performance of the Synthesized Inhibitor

As observed from Tables 1–6, the inhibitor exhibited a clear dose-dependent inhibition of scale formation across all tested temperatures (40°C, 60°C, and 70°C). At doses of 20–30 ppm, the inhibitor prevented visible scale formation for up to 24 hours, especially notable in Table 5 (CaCO₃ at 70°C), where the 30 ppm dose maintained a "Clear and Bright" (C,B) solution up to 24 hours. This confirms the thermal stability and functional performance of the synthesized compound in high-temperature environments typical of oilfield operations.

Chemical Confirmation and Structural Considerations

FT-IR, NMR (¹H and ¹³C), and mass spectrometry analyses (Figures 5–11) confirmed the successful substitution of guanidine with three phosphonate groups. However, only partial substitution (three out of five potential hydrogen sites) was achieved, likely due to steric hindrance and the stability of SP²N bonds, as discussed alongside Figure 8. This incomplete substitution, though a potential limitation, did not significantly impact the inhibitory performance, suggesting that three phosphonate groups were sufficient for high activity.

Compatibility and Biodegradability

Figure 4 illustrates excellent compatibility with calcium ions, as no precipitation was observed after 24 hours, even in the presence of 100 ppm Ca²⁺ and 3% NaCl. This is crucial for maintaining functionality in diverse brine conditions. Additionally, the biodegradability results, although not numerically detailed in the document, follow OECD 306 protocols. Given the oxygen consumption trends and background correction, the synthesized compound appears to meet environmentally favorable classification (likely "Green" or "Yellow"), although further confirmation with precise BOD values would strengthen this claim.

Comparative Context in Literature

Compared to traditional scale inhibitors such as BP-7 and BP-9, which suffer from low biodegradability and thermal limitations, the synthesized guanidine-based inhibitor represents an advancement. The molecule combines efficiency (as shown by titration results in Tables 7 and 8, where inhibition reached 100% at 30 ppm for both CaCO₃ and CaSO₄) with enhanced compatibility and presumed environmental safety. This places it among emerging "green" inhibitors that meet both performance and sustainability goals, addressing the gap noted in prior studies (Kelland, 2014; Mady & Kelland, 2017; Nowack, 2003).

Potential Sources of Error

Possible sources of error include:

- **Incomplete reaction substitution** during synthesis, as evidenced by spectroscopy, potentially affects consistency in scale inhibition.
- **Subjective assessment** of scale formation (e.g., "slight haze" vs. "moderate precipitate"), which could introduce variability in interpreting Table data.
- **Limited replicates** or absence of standard deviations for titration and biodegradability readings, which reduces statistical confidence in observed trends.

Future Considerations

Further optimization of reaction conditions (e.g., extending reaction time or using catalysts) might enable full substitution of guanidine hydrogens, potentially enhancing inhibitor strength. Moreover, detailed long-term reservoir simulation and toxicity profiling are essential next steps to validate the commercial viability of the synthesized compound.

CONCLUSION

This study successfully demonstrated the synthesis and evaluation of a novel guanidine-based scale inhibitor functionalized with phosphonate groups. The compound exhibited strong performance in preventing the formation of calcium carbonate and calcium sulfate scales across a range of temperatures, particularly at elevated conditions (up to 70°C). Spectroscopic analyses (FT-IR, NMR, and MS) confirmed the molecular structure of the synthesized compound, verifying the substitution of three hydrogen atoms in guanidine with phosphonate moieties.

Despite the incomplete substitution—likely due to steric hindrance and the chemical stability of SP² nitrogen—the inhibitor achieved high inhibition efficiency, with titration tests showing up to 100% inhibition at 30 ppm. The compound also demonstrated good compatibility with calcium ions and maintained clarity in brine solutions, suggesting its suitability for oilfield applications.

Furthermore, preliminary biodegradability results, aligned with OECD 306 guidelines, suggest the compound has potential for environmental acceptance, pending further detailed ecotoxicological assessments. Overall, the synthesized inhibitor represents a promising, cost-effective, and environmentally favorable alternative to conventional scale inhibitors, with potential for further development and application in high-temperature industrial systems.

ACKNOWLEDGEMENT

The authors would like to express their sincere gratitude to the Faculty of Pharmacy, University of Benghazi, for providing the necessary resources and support throughout the duration of this research. Special thanks are extended to the Libyan Academy for Postgraduate Studies for granting access to laboratory facilities and equipment essential for synthesis and performance testing.

We also acknowledge the National Research Center – Central Laboratory Services – Magnetic Resonance Laboratory in Cairo, Egypt, and the Libyan Advanced Center for Chemical Analysis in Tajoura, Tripoli, for their assistance with the NMR and FT-IR analyses, which were crucial to the structural characterization of the synthesized compound.

Our appreciation goes to all the technicians, supervisors, and collaborators who contributed to the success of this project through their technical expertise and continuous encouragement.

ETHICS

This research did not involve human participants, animal testing, or clinical trials. All experimental procedures were conducted in accordance with institutional safety and environmental guidelines. The use of chemicals and laboratory practices complied with standard ethical protocols, and all efforts were made to minimize environmental impact and ensure safe handling and disposal of reagents.

Duality of interest: The authors declare no conflict of interest

Author contributions: Contribution is equal between authors.

Funding: The authors did not receive any funding (institutional, private, and/or corporate financial support)

REFERENCES

- Ash, M. (2004). Handbook of green chemicals. Synapse Info Resources.
- Dakhil, O., Yahya, Y., Abdalkrim, H., & Eltawaty, S. (2022). Chemical Separation of Compounds from Antituberculosis Drug and Their Antibacterial Biological Activity. *AlQalam Journal of Medical and Applied Sciences*, 274-281.
- Delon Jimenez, P. (2014). *Improving squeeze scale inhibitor adsorption and flow back characteristics with surfactants* University of Stavanger]. http://hdl.handle.net/11250/222726
- Demadis, K. (2006). Investing in Chemical Cooling Water Treatment.
- Ebetino, F., Francis, M., Rogers, M., & Russell, R. (1998). Mechanisms of action of etidronate and other bisphosphonates. *Reviews in Contemporary Pharmacotherapy*, 9(4), 233-243.
- Garber, K. B., Vincent, L. M., Alexander, J. J., Bean, L. J., Bale, S., & Hegde, M. (2016). Reassessment of genomic sequence variation to harmonize interpretation for personalized medicine. *The American Journal of Human Genetics*, 99(5), 1140-1149.
- Hirabayashi, H., Sawamoto, T., Fujisaki, J., Tokunaga, Y., Kimura, S., & Hata, T. (2002). Dose dependent pharmacokinetics and disposition of bisphosphonic prodrug of diclofenac based on osteotropic drug delivery system (ODDS). *Biopharmaceutics & drug disposition*, 23(8), 307-315.
- Jordan, M., & Mackay, E. J. (2007). Scale Control in Chalk Reservoirs: The Challenge of Understanding the Impact of Reservoir Processes and Optimizing Scale Management by Chemical Placement and Retention—From the Laboratory to the Field. SPE Middle East Oil and Gas Show and Conference,
- Kelland, M. A. (2014). Production Chemicals for the Oil and Gas Industry.
- Kim, S.-H., Semenya, D., & Castagnolo, D. (2021). Antimicrobial drugs bearing guanidine moieties: A review. *European journal of medicinal chemistry*, 216, 113293.
- Kiran, Y., Reddy, C. D., Gunasekar, D., Reddy, C. S., Leon, A., & Barbosa, L. C. (2008). Synthesis and anticancer activity of new class of bisphosphonates/phosphanamidates. *European journal of medicinal chemistry*, 43(4), 885-892.
- Kukhar, V. P., & Hudson, H. R. (2000). *Aminophosphonic and aminophosphinic acids: Chemistry and biological activity*. John Wiley & Sons.
- Mady, M. F., & Kelland, M. A. (2017). Overview of the synthesis of salts of organophosphonic acids and their application to the management of oilfield scale. *Energy & Fuels*, 31(5), 4603-4615.
- Maeda, K. (2004). Metal phosphonate open-framework materials. *Microporous and mesoporous materials*, 73(1-2), 47-55.

- Moussa, A. (2014). Two Functional Guanidine Groups Are Responsible for the Biological Activity of Streptomycin and Functionally Equivalent Molecules. *J. Chromatogr. Sep. Tech*, *5*, 1-3.
- Nowack, B. (2003). Environmental chemistry of phosphonates. Water research, 37(11), 2533-2546.
- Popov, K., Kovaleva, N., Rudakova, G. Y., Kombarova, S., & Larchenko, V. (2016). Recent state-of-the-art of biodegradable scale inhibitors for cooling-water treatment applications. *Thermal Engineering*, 63(2), 122-129.
- Rodan, G. A., & Martin, T. J. (2000). Therapeutic approaches to bone diseases. *Science*, 289(5484), 1508-1514.
- Sparidans, R. W., Twiss, I. M., & Talbot, S. (1998). Bisphosphonates in bone diseases. *Pharmacy World and Science*, 20(5), 206-213.
- Woodward, G., Jones, C., & Davis, K. (2004). Novel Phosphonocarboxylic Acid Esters. *International Patent Application WO2004/002994*.
- Zamperini, C., Maccari, G., Deodato, D., Pasero, C., D'Agostino, I., Orofino, F., De Luca, F., Dreassi, E., Docquier, J.-D., & Botta, M. (2017). Identification, synthesis and biological activity of alkyl-guanidine oligomers as potent antibacterial agents. *Scientific reports*, 7(1), 8251.

Doi: https://doi.org/10.54172/qk3sra74

Research Article ⁶Open Access

Assessment of Radiation Hazards Parameters Associated with Natural Radionuclides in Granite Used in Al-Bayda, Libya



Jemila M. Ali^{1*}, Salah S. Basil¹ and Rabea A. Ammar²

- *Corresponding author: jemila.mussa@omu.edu.ly,
 Department of Physics, Faculty of Science, Omar AL-Mukhtar University, Libya.
- ¹ Department of Physics, Faculty of Science, Omar AL-Mukhtar University, Libya.
- ² Department of Physics, Faculty of Science, Sirt University, Libya.

Received: 02 May 2025

Accepted: 27 August 2025

Publish online: 31 August 2025

Abstract

The levels of natural radionuclides in granite samples used as building materials, collected from local markets in Al-Bayda, Libya, were investigated using a gamma ray spectrometer equipped with a NaI (Tl) scintillation detector. For ²²⁶Ra, ²³⁸U, ²³²Th, and ⁴⁰K, the respective activity concentrations ranged from 40.96±1.47 to 205.48±0.13 Bqkg⁻¹, 52.25 ± 1.53 to 182.65 ± 2.36 Bqkg⁻¹, 49.72 ± 1.17 to 144.32 ± 1.51 Bqkg⁻¹, and 49.41 ± 1.18 to 271.75 ± 2.74 Bqkg⁻¹. According to the data, all granite samples exhibited radioactive levels for ²²⁶Ra, ²³⁸U, and ²³²Th that exceeded the worldwide recommended limits set by UNSCEAR. Conversely, the activity concentration levels of ⁴⁰K in all granite samples were found to be below the UNSCEAR worldwide recommended values. The radiological hazard parameters associated with these natural radionuclides were subsequently evaluated. Comparison of the results with other global studies and world-recommended values revealed that while some parameters were lower than or within the recommended limits, others showed values higher than internationally accepted thresholds. Nevertheless, the findings indicate that for most of the studied granite samples, the radiation hazards from terrestrial radionuclides are within acceptable limits for their use as building materials.

Keywords: Natural Radioactivity; Granite Absorbed Dose Rate; Building Material; Annual Effective Dose.

INTRODUCTION

Natural radioactivity originates from terrestrial radioactivity and cosmic radiation. Humans primarily experience two types of exposure: internal exposure from inhaled radon-222 (²²²Rn) gas and its decay products, and external exposure from gamma rays emitted by terrestrial radionuclides like potassium–40 (40K) and the uranium (²³⁸U) and thorium (²³²Th) series (Sivakumar et al., 2014). Recent investigations in regions with high natural background radiation have raised awareness of risk assessment due to inhabitants' exposures to long-term low-level radiation (Akpanowo et al., 2020). These high radiation levels often stem from concentrated radio nuclides in granite rocks, soils, sediments, and other geological materials frequently used in construction and infrastructure (Abbasi, 2013). To accurately assess human exposure to natural radiation sources, it's crucial to understand public dosage limits and measure ambient background radiation levels from the ground, air, water, food, and within buildings (Kovacs et al., 2017). Consequently, information about the



The Author(s) 2025. This article is distributed under the terms of the *Creative Commons Attribution-NonCommercial 4.0 International License* (http://creativecommons.org/licenses/by-nc/4.0/), which permits unrestricted use, distribution, and reproduction in any medium, *for non-commercial purposes only*, provided you give appropriate credit to the original author(s) and the source, provide a link to the Creative Commons license, and indicate if changes were made.

concentrations of these radio nuclides in the environment is fundamental for estimating the level of public exposure to ionizing radiations (Lee et al., 2019). Currently, there is limited information available concerning the radioactive levels of building materials in Libya. Therefore, determining the activity concentrations of these materials is necessary to evaluate potential radiological risks to building inhabitants (Hanfi et al., 2022). This study aims to determine the natural radioactivity in granite samples, commonly used as building materials in Al-Bayda, Libya, by utilizing a gamma spectrometer to measure the activity concentrations of ²²⁶Ra, ²³⁸U, ²³²Th, and ⁴⁰K.

MATERIALS AND METHODS

Sampling Collected and Preparation

In this study, gamma-ray spectroscopy with a sodium iodide thallium-doped NaI (Tl) detector with a "1.5×1.5" crystal, model No. PM-9266B, serial No. WA00012638. The detector was encased within a lead shield of sufficient thickness to minimize background radiation contributions from cosmic rays and ambient laboratory sources. Gamma spectra acquisition and subsequent analysis were performed utilizing the Cassy Lab software system. The activity concentrations of the ²³⁸U and ²³²Th decay series and ⁴⁰K were determined in 13 granite samples imported from India, which are commonly used as building materials and decorative materials in the city of Al-Beida, Libya. The solid samples were pulverized into a fine powder and passed through a standard 2 mm sieve, and then the samples were dried at a temperature of 110°C for two hours in an oven used to remove any moisture and achieve homogeneity. Before being analyzed using a gamma spectrometer, the samples were weighed and placed in 250 cm³ polyethylene containers, weighed, and stored for more than 30 days to reach equilibrium in the radioactivity between ²³⁸U and ²³²Th and their corresponding daughters. In order to ensure that the daughter remains in the sample and that the radon gas is contained inside the volume, this step is necessary. For gamma analysis, these samples were placed directly above the detector. The counting time for each sample was 7200 seconds. Figures 1) show gamma ray spectroscopy.



Figure: (1). The gamma spectroscopy system.

Calculations of Radioactivity Concentration Level

Concentration of activity (A) The rate at which an isotope decays is known as the radioactivity of a radioactive source. The quantity of radiation produced over time can be thought of as "radioactivity. Gamma spectroscopy measurements of each peak were used to determine the radioactivity levels of the different radionuclides that had been identified. The formula below was used to determine the associated activity (A) (Orosun et al., 2020).

$$A = \frac{(CPS)}{I \quad \xi \cdot M} \tag{1}$$

Where: CPS: the energy-related net counts per second.

I: is the probability of gamma ray emission at the energy peak, ε : the absolute efficiency at photopeak energy, M: the sample's mass in kg, T: is the sample spectrum collection time (sec).

Calculations of Radiological Parameters Radium Equivalent

The equivalent radioactivity, the radiation index evaluates a material's suitability for construction using the assumption that the gamma dose rates produced by 370 Bqkg⁻¹of ²²⁶Ra, 259 Bq kg-1 of ²³²Th, and 4810 Bq kg-1 of ⁴⁰K are equal. To determine the radium equivalent activity, use the formula:

$$Ra_{eq} = A_{Ra} + (1.43 A_{th}) + (0.077 A_k)$$
 (2)

Where: A_{Ra} , A_{Th} , and A_k , represent the specific activity concentrations of 226 Ra, 232 Th, and 40 K, for safe use building materials should not exceed 370 Bq kg-1 (Agora and Hashim, 2015; Ahmed Etal. ,2022).

Gamma Radiation Level Index

Gamma radiation index I_r is used to estimate the level of gamma radiation hazard associated with the natural radionuclides in building materials. It is identifying materials that may be hazardous to health when used for the construction of buildings. I_r calculated using an equation based on (Mahmoud et al., 2020):

$$I_{\gamma} = \frac{A_{R\alpha}}{150} + \frac{A_{Th}}{100} + \frac{A_{K}}{1500} \tag{3}$$

Alpha Index

There is an association between alpha particle indices and radon inhalation from construction materials. The index of alpha is calculated using the relation (El-Feky et al., 2022):

$$I_{\alpha} = \frac{A_{R\alpha}}{200} \tag{4}$$

Internal Hazard Index

The internal radiation hazard index (H_{in}) provides an estimate of radon exposure and its daughter product, which is defined as (Alaboodi et al., 2020).

$$H_{in} = \frac{c_{R\alpha}}{185} + \frac{c_{Th}}{259} + \frac{c_K}{4810} \le 1 \tag{5}$$

The External Hazard Index Hex

The external hazard index H_{ex} is the assessment of the hazard of γ -radiation. The Hex values are detected via the following formula (Najam et al., 2015):

$$H_{ex} = \frac{A_{R\alpha}}{370} + \frac{A_{Th}}{259} + \frac{A_K}{4810} \le 1 \tag{6}$$

Gamma Absorbed Dose Rate

The absorbed dose rate D_R (nGyh⁻¹) due to terrestrial gamma rays at 1 m above the ground according to the activity concentrations of ²²⁶Ra, ²³²Th, and ⁴⁰K in the granite samples, was

determined using the equation (Mansor et al., 2020):

$$D_{R} = 0.462 A_{Rd} + 0.604 A_{th} + 0.042 A_{K}$$
 (7)

The Annual Effective Dose Rate

In order to establish the annual effective dose rate in the air, the conversion coefficient between the absorbed dose in the air and the effective dose received by an adult must be considered. This value for environmental exposure to gamma rays with moderate energy is 0.7 SvGy⁻¹, according to UN-SCEAR(2000). The occupancy factor for indoor measurements is about 0.8, as is the case for building materials, and the indoor annual effective dose equation becomes:

$$E_{in} (\text{mSvy}^{-1}) = D_R(\text{nGyh}^{-1}) \times 8760 (\text{hy}^{-1}) \times 0.8 \times 0.7 (\text{SvGy}^{-1}) \times 10^{-6}$$
(8)

There is about a 0.2 outdoor occupancy factor. Equation (9) gives the outdoor annual effective dose equivalent (Darwish et al., 2015)

$$Eout(mSvy^{-1}) = DR (nGyh-1) \times 8760 (hy^{-1}) \times 0.2 \times 0.7 (SvGy^{-1}) \times 10^{-6}$$
 (9)

Excess Lifetime Cancer Risk (ELCR)

A person's risk of acquiring cancer increases with radiation exposure during their lifetime. ELCR was determined from the formula below:

$$ELCR = E_{out} \times DL \times RF \tag{10}$$

Where, according to the ICRP (2012), RF is a constant risk factor that is distributed to the community at a rate of 0.05 Sv (Taskin et al., 2009), DL is the life expectancy (70 years), and E_{out} is the outdoor annual effective dose equivalent (Yalcin et al., 2020).

RESULTS

The specific activity concentration values are recorded in Table (1). The values for radionuclides varied from 40.96 ± 1.47 to 205.48 ± 0.13 , 52.25 ± 1.53 to 182.65 ± 2.36 , 49.72 ± 1.17 to 144.32 ± 1.51 , and 49.41 ± 1.18 to 271.75 ± 2.74 Bq kg⁻¹ for ²²⁶Ra, ²³⁸U, ²³²Th, and ⁴⁰K, respectively, with an average of 119.88 ± 1.61 , 121.94 ± 2.49 , 97.17 ± 1.85 , and 169.97 ± 2.46 Bq kg⁻¹, respectively, as shown in Figure (2).

Table ((1)):The s	pecific	activity co	oncentrations	(Bakg	·1) (of the	radio	nuclides	in th	ne investi	gated	samples.

Sample No.	²²⁶ Ra	²³⁸ U	²³² Th	⁴⁰ K
G1	100.98±1.74	86.00±1.78	116.46±1.36	126.27±1.87
G2	40.96±1.47	52.25±1.53	55.39±1.22	111.17±1.76
G3	117.93±1.80	116.95±1.78	69.34±1.13	131.76±1.91
G4	134.17±1.86	182.65±2.36	63.93±1.05	57.64±1.27
G5	144.05 ± 1.90	94.22±1.88	127.29±1.56	52.15±1.21
G6	136.99±1.88	127.98±2.06	112.78 ± 1.47	82.35±1.52
G7	165.94±1.98	156.7±2.27	65.98±1.14	49.41±1.18
G8	127.81 ± 1.84	119.69 ± 2.04	90.61±1.32	116.66±1.80
G9	60.02±1.56	72.87±1.71	72.51±1.83	111.17±1.76
G10	135.58±1.44	160.31±1.38	144.32±1.51	68.62±0.71
G11	205.48 ± 0.13	182.24±9.94	100.44 ± 7.39	223.71±12.39
G12	122.87±1.82	99.36±1.99	105.30 ± 1.92	271.75 ± 2.74
G13	65.67±1.59	94.32±1.68	49.72±1.17	126.27±1.87
Average	119.88±1.61	121.94 ± 2.49	97.17±1.85	169.97 ± 2.46
P. L.	50	50	50	500

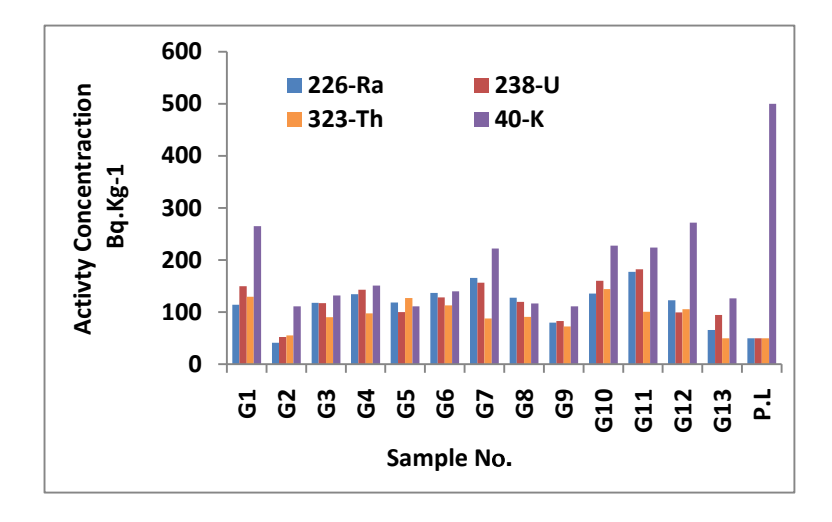


Figure (2). The specific activity concentrations of granite samples.

The average values of activity concentrations of radionuclides in the samples under study exceeded the globally recommended limit values of 50, 50, and 50 Bqkg⁻¹ for radionuclides ²²⁶Ra, ²³⁸U, and ²³²Th, respectively (UNSCEAR, 2010). However, the calculated mean value for ⁴⁰K was lower than the 500 Bqkg⁻¹ worldwide mean (UNSCEAR, 2010). The radiological hazards caused by exposure due to radionuclides were presented in Tables (2).

Tables (2): The radiological hazard parameters in investigation samples.

Sample			Hazard indico	es	D_R	E_{in}	E_{out}	ELCR	
No.	R_{aeq}	I_{γ}	I_{α}	H_{in}	H_{ex}	- (nGy.h ⁻¹)	(msv.y ⁻¹)	(msv.y ⁻¹)	× 10 ⁻³
G1	320.08	1.12	0.57	1.17	0.86	142.24	0.70	0.17	0.57
G2	128.72	0.45	0.20	0.46	0.35	57.04	0.27	0.06	0.23
G3	256.87	0.89	0.59	1.01	0.69	114.42	0.56	0.14	0.46
G4	284.98	0.98	0.67	1.13	0.77	127.12	0.62	0.16	0.51
G5	309.21	1.07	0.59	1.16	0.83	136.36	0.67	0.17	0.55
G6	309.04	1.06	0.68	1.20	0.83	137.29	0.67	0.17	0.55
G7	308.86	1.07	0.83	1.28	0.83	139.14	0.68	0.17	0.56
G8	266.37	0.92	0.64	1.06	0.72	118.68	0.58	0.14	0.48
G9	192.05	0.67	0.40	0.73	0.51	85.33	0.42	0.10	0.34
G10	359.50	1.24	0.68	1.34	0.97	159.38	0.78	0.19	0.64
G11	338.09	1.17	0.89	1.39	0.91	151.94	0.74	0.19	0.61
G12	294.37	1.03	0.61	1.13	0.79	131.78	0.65	0.16	0.53
G13	146.49	0.51	0.33	0.57	0.40	117.74	0.58	0.14	0.48
Average	269.43	0.93	0.59	1.04	0.72	124.49	0.60	0.13	0.50
P. L	370	1	1	1	1	84	1	0.07	0.29

The results of the Ra_{eq} values calculated for the granite samples ranged from 128.72 to 359.50 Bq kg⁻¹, with an average value of 269.43 Bqkg⁻¹. The obtained values in this study are lower than the world-recommended value of 370 Bqkg⁻¹ (UNSCEAR, 2010). The values obtained of I_r for samples ranged from 0.45 to 1.24, with an average value of 0.93. These results indicate that the gamma

radiation index exceeded the recommended value of 1 (UNSCEAR, 2010) for most samples. For I_a, the result ranged from 0.20 to 0.89 with an average value of 0.59. Consequently, the value of the internal hazard index ranged from 0.46 to 1.39, with an average value of 1.04. The values of most samples exceed the recommended limit of 1 (UNSCEAR, 2010), and some individual samples also showed values above this limit. Also, the values of the external hazard index ranged from 0.35 to 0.97, with an average value of 0.72. The results showed that H_{ex} values for all studied samples are lower than unity (UNSCEAR, 2010). On the other hand, the absorbed dose rate ranges from 57.04 to 159.38 nGyh⁻¹, but the average absorbed dose rate value for granite samples was 124.49 nGyh⁻¹. This average is higher than the world-recommended value of 84 nGyh⁻¹ (UNSCEAR, 2010), with the exception of sample G2, which showed a lower value. The values of the indoor annual effective dose varied from 0.27 to 0.78 mSvy⁻¹, with an average value of 0.60 mSv y⁻¹. The average values for all measured samples were less than the 1 mSvy⁻¹ limit (UNSCEAR, 2017, and Muyiwa et al., 2020). The outdoor annual effective dose ranged from 0.06 to 0.19 mSvy⁻¹ with an average value of 0.13 mSvv⁻¹. These values of E_{out} are higher than the recommended value of 0.07 mSvv⁻¹ (UN-SCEAR, 2010). The recorded values for ELCR range from 0.23 to 0.64 with an average value of 0.50. For all samples, these values were higher than the recommended world value of 0.29 \times 10⁻³ (UNSCEAR, 2010). The current study will be compared with some previous studies, as shown in Tables (3)

Table (3): Comparison of radiological hazard indices in present work with those in other countries of the world.

	Hazar	d index			D_R		effective nSvy ⁻¹)	ELCR	Ref.	
Ra _{eq} (Baka-1)	I_{γ}	I_{α}	H_{in}	H_{ex}	(nGyh ⁻¹)	E_{in}	E_{out}	×10 ⁻³		
251.87	0.87	0.48	0.94	0.67	111.62	0.54	0.13	0.45	Present work	
1016.92	8.29	-	3.03	2.75	534.42	-	-	-	(Sroor, 2013)	
487	1.87	-	_	1.2	261	-	-	-	(Obaid et al., 2015)	
176	0.67	0.19	0.58	0.48	160	-	-	-	(Imani et al., 2021)	

CONCLUSIONS

This study systematically assessed the natural radioactivity levels in granite samples utilized as building materials in Al-Beida, Libya. The investigation revealed that while 40 K activity concentrations were below globally recommended values, the concentrations of 226 Ra, 238 U, and 232 Th exceeded established acceptable limits. Regarding radiological hazard parameters, most samples exhibited higher than world-average recommended values for the gamma radiation index (I_r), internal hazard index (H_{in}), absorbed dose rate, and lifetime cancer risk. Consequently, the outdoor annual effective doses for all studied granite samples were also higher than the world-recommended value. These results are crucial for enhancing the database on natural radioactivity in Libyan construction materials, which will facilitate further risk assessment and contribute to awareness efforts for mitigating hazardous material exposure.

ACKNOWLEDGEMENT

We do not have any financial support or relationships that may pose a conflict of interest in the cover letter submitted with the manuscript.

Duality of interest: The authors declare that they have no duality of interest associated with this manuscript.

Author contributions: A.B and C developed theoretical formalism, performed the analytic calculations, and performed the numerical simulations. Both A.B and C. authors contributed to the final version of the manuscript. A.C. supervised the project.

Funding: No specific funding was received for this work.

REFERENCES

- Abbasi, A. (2013). *Environmental radiation in high exposure building materials*. Eastern Mediterranean University (EMU)-Doğu Akdeniz Üniversitesi (DAÜ).
- Ahmed S. E. A., Jemila M. A. and Salah S. Basil. (2022). Concentration of Naturally Radioactive Elements in Rocks and Its Radiological Risk around Al-Bayda City, Libya. *Special Issue for 5th International Conference for Basic Sciences and Their Applications*; 19(2): 102-112.
- Akpanowo, M.A., Umaru, I., Iyakwari, S., Joshua, E.O., Yusuf, S. and Ekong, G.B. (2020) Determination of Natural Radioactivity Levels and Radiological Hazards in Environmental Samples from Artisanal Mining Sites of Anka, North-West Nigeria. *Scientific African*, 10, 1-11, e00561. https://doi.org/10.1016/j.sciaf.2020.e00561
- Alaboodi, A., Kadhim, N., Abojassim, A., & Hassan, A. B. (2020). Radiological hazards due to natural radioactivity and radon concentrations in water samples at Al-Hurrah city, Iraq. *International Journal of Radiation Research*, 18(1), 1-11.
- Darwish, D., Abul-Nasr, K., & El-Khayatt, A. (2015). The assessment of natural radioactivity and its associated radiological hazards and dose parameters in granite samples from South Sinai, Egypt. *Journal of Radiation Research and Applied Sciences*, 8(1), 17-25.
- El-Feky, M. G., Taha, S. H., El Minyawi, S., Sallam, H., Tawfic, A., Omar, A., & El-Samrah, M. (2022). *Radioactivity and environmental impacts of granites from um Ara, southeastern desert, Egypt.* Paper presented at the Journal of Physics: Conference Series .https://dioi.10.1088/1742-6596/2305/1/012033
- Gaafar, I., Elbarbary, M., Sayyed, M., Sulieman, A., Tamam, N., Khandaker, M. U., . . . Hanfi, M. Y. (2022). Assessment of radioactive materials in albite granites from abu rusheid and um naggat, central eastern desert, Egypt. *Minerals*, 12(2), 120. https://doi.org/10.3390/min12020120
- Kovacs, T., Bator, G., Schroeyers, W., Labrincha, J., Puertas, F., Hegedus, M., . . . Grubeša, I. (2017). From raw materials to NORM by-products *Naturally occurring radioactive materials in construction* (pp. 135-182): Elsevier.
- Lee, K. Y., Hwang, S., Kim, Y., & Ko, K.-S. (2019). Measurement of NORM in geologic and building materials by pair measurement–gamma spectrometry. *Journal of Radioanalytical and Nuclear Chemistry*, 322(3), 1791-1795. https://doi:10.1007/s10967-019-06896-w
- Mahmoud, M. A., & Abd El-Halim, E. S. (2020). Radiological Impact of Natural Radioactivity in White Granite at Um Baanib area, Southeastern Desert, Egypt. *Arab Journal of Nuclear Sciences and Applications*, 53(1), 1-8. https://doi:10.21608/ajnsa.2019.5051.1117

- Mansor, M. A., & Rashid, J. M. (2020). Evaluation of natural radioactivity for building materials samples used in tall Al Ubaid archaeologist in Dhi-Qar governorate-Iraq. *Samarra Journal of Pure and Applied Science*, 2(1), 53-66.
- Najam, L. A., Tawfiq, N. F., & YOUNIS, A. (2015). Measurement of natural radioactivity in brick samples used in the construction in Iraq. *Arch Phys Res*, 6(1), 13-19.
- Orosun, M. M., Usikalu, M. R., Oyewumi, K. J., & Achuka, J. A. (2020). Radioactivity levels and transfer factor for granite mining field in Asa, North-central Nigeria. *Heliyon*, 6(6). https://doi:10.1016/j.heliyon.2020.e04240
- Orosun, M. M., Usikalu, M. R., Oyewumi, K. J., & Achuka, J. A. (2020). Radioactivity levels and transfer factor for granite mining field in Asa, North-central Nigeria. *Heliyon*, 6(6). https://doi: 10.1016/j.heliyon.2020.e04240.
- Sivakumar, S., Chandrasekaran, A., Ravisankar, R., Ravikumar, S., Prince Prakash Jebakumar, J., Vijayagopal, P., . . . Jose, M. (2014). Measurement of natural radioactivity and evaluation of radiation hazards in coastal sediments of east coast of Tamilnadu using statistical approach. *Journal of Taibah University for Science*, 8(4), 375-384. https://doi: 10.1016/j.jtusci.2014.03.004
- Taskin, H., Karavus, M., Ay, P., Topuzoglu, A., Hidiroglu, S., & Karahan, G. (2009). Radionuclide concentrations in soil and lifetime cancer risk due to gamma radioactivity in Kirklareli, Turkey. *Journal of environmental radioactivity, 100*(1), 49-53. https://doi: 10.1016/j.jenvrad.2008.10.012
- UNSCotEoA, R., & Annex, B. (2000). Exposures from natural radiation sources. New York, United Nation.
- UNSCEAR (2010). Sources And Effects Of Ionizing Radiation.(2008 Report. Volume Ii: Effects. Scientific Annexes C, D And E. New York, Usa: United Nations Scientific Committee On The Effects of Atomic Radiation. Available From: http://www.unscear.org/Docs/Publications/2008/Unscear_2008_Report_Vol.Ii.Pdf.
- Yalcin, F., Unal, S., Yalcin, M. G., Akturk, O., Ocak, S. B., & Ozmen, S. F. (2020). Investigation of the effect of hydrothermal waters on radionuclide activity concentrations in natural marble with multivariate statistical analysis. *Symmetry*, 12(8), 1219. https://doi.org/10.3390/sym12081219

Doi: https://doi.org/10.54172/h2qgcx97

Research Article ⁶Open Access

Determination of lead Element in Hair Dye Samples Available in Libyan Markets Using Atomic Absorption Spectroscopy



Elham Alterhoni¹, Mona H. Ali Bnhmad²*, Rabia Omar Eshkourfu³, Amina Mohamed Amimn¹, Ebtihaj Abdul Aziz Youssef¹, Ebtihal Mustafa Al-Zurqani¹, Aya Al-Hadi Ebrahim¹, and Afaf Ali Al-Rutbi¹

- ¹ Department of Pharmaceutical Chemistry, Faculty of Pharmacy, Elmergib University, Al Khums, Libya.
- ² Chemistry Department, Faculty of Arts and Sciences, Al-Marj, University of Benghazi, Libya.
- ³ Department of Chemistry, Elmergib University, AL-Khums, Libya

*Corresponding author: mona.bnhmad@uob.edu.ly Chemistry Department, Faculty of Arts and Sciences, Al-Marj, University of Benghazi, Libya.

Received:

09 May 2025

Accepted:

30 August 2025

Publish online:

31 August 2025

Abstract

Hair dyes are essential to cosmetic products; however, they may contain harmful chemicals that pose health risks when used repeatedly. This study analyzed six commercial hair dye samples available in the Libyan markets, representing multiple colors (black, blonde and brown) to ensure a comprehensive assessment. Advanced analytical techniques, specifically Atomic Absorption Spectroscopy (AAS), were employed to determine the lead concentration in the samples. Random samples were selected from the markets for analysis, and the results revealed that most samples had undetectable levels of lead (<0.1 µg/L) for samples 1 to 3. However, sample 4 exhibited a significant lead concentration, with an average value of 12.92 µg/L, ranging from 10.2 µg/L to 14.56 µg/L. Samples 5 and 6 were also free from detectable lead. This study emphasizes the importance of continuous monitoring of cosmetic products, particularly regarding heavy metals that could pose public health risks. The findings suggest that some products contain elevated lead levels, highlighting the need for preventive measures to ensure consumer safety. Additionally, the study calls for increased consumer awareness of the risks of lead exposure and the importance of selecting safe products.

Keywords: Hair Dyes, Lead, Atomic Absorption Spectroscopy (AAS), Heavy Metals.

INTRODUCTION

Heavy metals, especially lead, are considered as a major environmental and health hazards. Lead exposure can occur through various sources; including contaminated air, water, soil, food, and consumer products. In particular, cosmetic products such as hair dyes are increasingly scrutinized due to the potential presence of harmful substances like lead, which can be absorbed through the skin and cause serious health effects. Chronic exposure to lead is known to adversely affect the nervous system, kidneys, and reproductive system, particularly in vulnerable populations such as children, pregnant women, and those with pre-existing health conditions (Bellinger, 2017; World Health Organization, 2019).

Lead is classified as a neurotoxin and its presence in personal care products especially those



The Author(s) 2025. This article is distributed under the terms of the *Creative Commons Attribution-NonCommercial 4.0 International License* ([http://creativecommons.org/licenses/by-nc/4.0/] (http://creativecommons.org/licenses/by-nc/4.0/]), which permits unrestricted use, distribution, and reproduction in any medium, *for non-commercial purposes only*, provided you give appropriate credit to the original author(s) and the source, provide a link to the Creative Commons license, and indicate if changes were made.

applied directly to the skin, is a significant public health concern. Although various studies indicate the presence of heavy metals, including lead, in cosmetic products globally (Hussein et al., 2020; Ugochukwu et al., 2021), the situation in developing countries, such as Libya, remains underexplored. Given that the cosmetics market in Libya has seen significant growth over the past few decades, it is crucial to assess the safety of products available to consumers (Rasool et al., 2016). The Atomic Absorption Spectroscopy (AAS) is one of the most reliable techniques for detecting and quantifying trace elements such as lead in various samples, including cosmetics. AAS has become the standard method for heavy metal analysis due to its sensitivity, precision, and ability to detect low concentrations (Cohen et al., 2022; Chojnacka et al., 2005).

This study aims to determine the concentration of lead in some imported hair dye samples available in Libyan markets using AAS. The research will contribute to filling the gap in knowledge regarding the safety of cosmetic products in Libya and will help raise awareness about the potential risks posed by lead contamination in such products.

MATERIALS AND METHODS

T Materials

Six samples of hair dye, concentrated nitric acid HNO₃ (69.5% for Carlo Erba analysis) were used to digest the samples, and distilled water.

Equipment Apparatus

Atomic Absorption Spectrometer (AAS), Filtration equipment (filter paper, funnel, etc.), graphite furnace type Varian-USA

Sample Collection

Six dye samples were collected from different stores in the Libyan market. The selected dye types were among the most common types used by consumers in the markets.

Preparation of Sample

- 1. To prepare the sample for lead analysis, approximately 1-2 g of the hair dye sample is accurately weighed into a clean, heat-resistant crucible. The sample is then ignited in a muffle furnace at 550°C for 2-3 hours to ensure complete combustion, converting all elements into their oxide forms and removing any organic matter. After cooling, the ash is transferred into a beaker, and a few milliliters of concentrated nitric acid (HNO₃) are added to dissolve the ash and release the lead content into the solution. The solution is gently heated in a fume hood to ensure complete digestion of the ash, as vapors from the nitric acid are released during this process (Cohen, J., Smith, T., & Davis, R. 2022)
- 2. Once digestion is complete and the solution becomes clear, it is filtered through filter paper to remove any insoluble particles, such as remaining ash or unreacted materials. The filtered solution is then transferred into a volumetric flask and diluted with distilled water to a final volume of 50 mL. This dilution ensures that the lead concentration falls within the measurable range for Atomic Absorption Spectroscopy (AAS).
- 3. For the blank solution, a clean crucible is ignited in the muffle furnace at 550°C for 2-3 hours to remove any organic matter. After cooling, a small volume of concentrated nitric acid is added to the crucible and gently heated to digest the acid. After digestion, the acid is directly

transferred into a clean beaker and then diluted with distilled water to a 50 mL volume. This blank solution is essential to account for any potential interference or contamination from the reagents during the lead determination process (ASTM International, 2022).

RESULTS

Calibration curve of lead standard

The standard linear calibration curve was obtained from the analysis of standard solutions (Table 1). It showed a relationship between the absorbance and concentrations of the standard solutions (Figure 1).

Table (1). Relationship between the concentration and the absorption of lead.

Concentration	Absorbance				
0	0				
0.01	0.01				
0.02	0.015				
0.04	0.029				

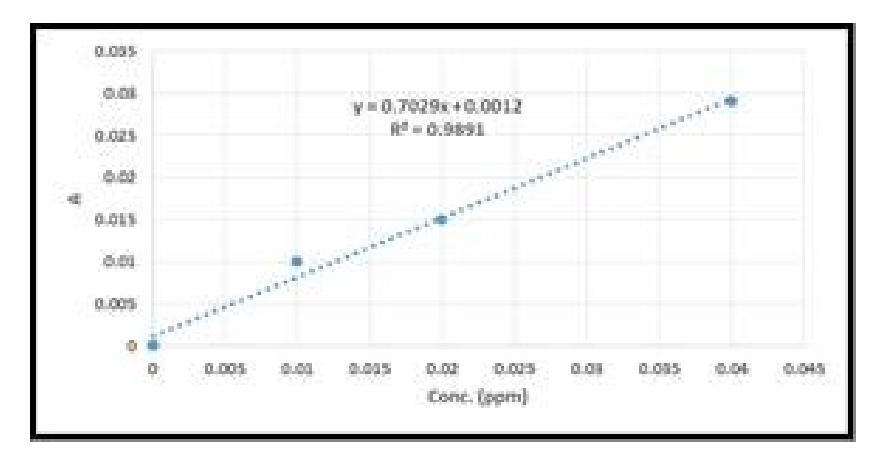


Figure (1). The calibration curve of lead.

Table (1) shows the relationship between each concentration of lead and its absorption value. This relationship can also be observed in Figure (1) on a linear scale. As a result, the concentration of metal content (mg/Kg) can be calculated (Bnhmad, Mona et al., 2024).

Table (2). Concentration of lead in hair dye.

Samples	R1	R2	R3	$Average(\mu g/L)$
1	< 0.1	< 0.1	<0.1	<0.1
2	< 0.1	< 0.1	< 0.1	< 0.1
3	< 0.1	< 0.1	< 0.1	< 0.1
4	14.56	10.2	14	12.92
5	< 0.1	< 0.1	< 0.1	< 0.1
6	< 0.1	< 0.1	<0.1	<0.1

The analysis of hair dye samples available revealed that the majority of the samples contained lead concentrations below the detection limit ($<0.1 \mu g/L$), except sample 4, which exhibited significantly higher levels of lead ($12.92 \mu g/L$ on average).

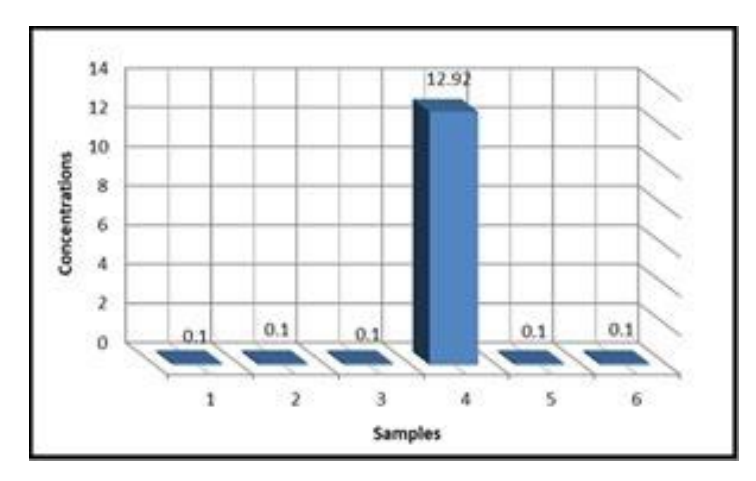


Figure (2). Concentration of lead in hair dye

DISCUSSION

The measurements presented in table (2) show that the concentrations of lead (Pb) in hair dye samples were mostly below the detection limit ($<0.1 \,\mu g/L$) for most of the samples (samples 1, 2, 3, 5, and 6). However, for sample 4, the concentration is significantly higher, with values of (12.92 $\,\mu g/L$).

The significant increase in lead levels in sample 4 could be attributed to several factors: Hair dyes may contain ingredients sourced from various raw materials, some of which may be contaminated with lead. Lead can enter the formulation of dyes if used in certain steps of processing or if raw materials are contaminated. Studies have shown that various industrial processes, particularly in countries with weaker regulatory frameworks, can unintentionally introduce heavy metals like lead into consumer products (Vargas et al., 2014).

Some hair dyes, especially older formulations, may contain lead acetate or lead-containing compounds to enhance the coloring effect. Lead acetate, in particular, has been used in hair dyes as a colorant and in some darkening products. While the use of lead acetate has been restricted in many countries, it might still be found in certain products, especially those imported from regions with less stringent regulations (U.S. Food and Drug Administration, 2020). This might explain the elevated levels in sample 4 if it contains lead-based pigments that were not properly regulated or disclosed on the product label.

Lead contamination can also occur due to environmental factors; for example, the exposure of hair dye products to lead-contaminated surfaces or containers during transportation or storage could result in trace amounts of lead being incorporated into the product. Such contamination could be more significant if the products were stored in older facilities or transported using materials that were previously in contact with lead-based substances (Kaur et al., 2015).

It is possible that sample 4 was imported from a different batch or manufacturer, which could have influenced the level of lead contamination. Variations in the source of raw materials, quality control processes, and manufacturing facilities could explain why sample 4 has elevated lead levels while other samples remain below detection limits.

Lead is a regulated substance in consumer products like hair dye; for example, the European Union (EU) restricts the use of lead in cosmetics to a maximum of $0.5 \,\mu\text{g/g}$ in finished products (European Commission, 2019). If sample 4 violates these standards, this could suggest that it either came from an unregulated source or failed to meet the safety guidelines enforced by authorities.

CONCLUSION

In this study, the findings suggest that while most products are free from detectable lead contamination, certain hair dye products may contain elevated lead levels due to various factors such as contamination during manufacturing, the use of lead-based pigments, environmental contamination, or differences in manufacturing processes.

Although the presence of lead was minimal in most samples, even small amounts of lead can pose health risks, especially with prolonged or repeated exposure.

To improve consumer safety, it is important to strengthen regulations on heavy metals in cosmetics, particularly lead, by aligning with international standards. Public awareness campaigns should educate consumers on the risks of lead exposure and encourage the selection of safe products. Additionally, regular testing of cosmetics, especially imports, is necessary to ensure safety.

Duality of interest: The authors declare no conflict of interest

Author contributions: Contribution is equal between authors.

Funding: The authors did not receive any funding (institutional, private, and/or corporate financial support)

REFERENCES

- ASTM International. (2022). ASTM D4975-22: Standard test method for lead in paint by atomic absorption spectroscopy. ASTM International.
- Bellinger, D. C. (2017). Lead neurotoxicity and the developing brain: Implications for the prevention of neurodevelopmental disorders. *Environmental Health Perspectives*, 125(4), 451-457.
- Bnhmad, M. H. A., Alterhoni, E., benhamad, O., & Amimn, A. M. (2024). Estimate of Sodium Benzoate Preservative in Some Soft Drinks in Local Markets in Libya Using a UV-Spectrometer. *Tarbawe Journal*. 24, 189-193. http://tarbawej.elmergib.edu.ly.
- Chojnacka, K., Górecka, H., Chojnacki A., and Górecki, H. (2005) Inter-element interactions in human hair. *Environ Toxicol Pharmacol*, vol. 20, no. 2, pp. 368–374.
- Cohen, J., Smith, T., & Davis, R. (2022). Application of Atomic Absorption Spectrometry in the analysis of heavy metals in personal care products. *Journal of Environmental Analytical Chemistry*, 45(2), 134-145.
- European Commission. (2019). Regulation (EC) No 1223/2009 on cosmetic products. *Official Journal of the European Union*.
- Hussein, S. A., Al-Kahtani, S. A., & Rahman, M. A. (2020). Heavy metals in cosmetics: Sources, exposure routes, and health effects. *Environmental Toxicology and Pharmacology*, 74, 103332.

- Kaur, M., & Prakash, S. (2015). Environmental contamination by heavy metals in cosmetic products. *Environmental Toxicology and Pharmacology*, 39(3), 1122-1129. [DOI: 10.1016/j.etap.2015.02.006]
- Rasool, S. R., Al-Dahhan, W., Al-Zuhairi, A. J., F., Hussein, Rodda, K. E., and Yousif E. (2016) Fire and Explosion Hazards expected in a Laboratory, *J Lab Chem Educ*, vol. 4, no. PNNL-SA-118942.
- U.S. Food and Drug Administration. (2020). Lead in Cosmetics. Retrieved from FDA.gov
- Ugochukwu, M. I., Ogbu, C. A., & Ogbunugafor, H. A. (2021). Assessment of lead and other heavy metals in commercial hair dye products in Nigeria. *Environmental Monitoring and Assessment*, 193(4), 219.
- Vargas, L., Rojas, J., Rodríguez, M., & Sáez, M. (2014). Heavy metal contamination in personal care products. *Journal of Environmental Science and Health*, Part A, 49(9), 987-993. DOI: 10.1080/10934529.2014.922045.
- World Health Organization. (2019). Lead exposure and health. World Health Organization.

Doi: https://doi.org/10.54172/tbjewm86

Research Article ⁶Open Access

Some Types of near Normality Based on Soft Simply Open Sets



Rukaia M. Rashed

*Corresponding author:: r.rasheed@zu.edu.ly, Department of Mathematics, Faculty of Education, Al-Zawia University, Libya.

Received: 21 May 2025

Accepted: 26 August 2025

Publish online: 31 August 2025

Abstract

This study investigates the fundamental properties and applications of soft simply open sets within soft topological spaces. We establish novel theoretical frameworks by:

- 1- Characterizing their relations to soft separation axioms (particularly near normality).
- 2- Demonstrating their duality through soft, simply interior (closure) operations, and proving their efficacy in handling uncertain data structures.

The results highlight how soft simply open sets bridge theoretical topology with computational applications, offering new tools for complex data analysis. Future directions include extensions to soft compactness and connection with fuzzy neural networks.

Keywords: Soft Sets, Soft Topology, Soft Simply Open Set, Soft Simply Normal, Soft Simply-Exterior, Soft Simply-Boundary.

INTRODUCTION

Soft set notion was introduced, for the first time, by (Molodtsov 2017) as mathematical models in order to deal with vagueness and sets to solve complicated problems in fields such as computer sciences, medical sciences, economics, and engineering, among others. Moreover, he studied the main points of this theory and its properties.

Shabir et al. (Shabir 2011) introduced and studied the concept of soft topological spaces, which are defined over an initial universe with a fixed set of parameters.

After that, many researchers (Arockiaran, Chen 2013; Hussain, Min, Nazmul 2013; Zorlutuna 2013) added several notions and concepts towards (Maji 2003, Min 2011; Molodtsov 1999; Zorlutuna 2012) the properties of soft topological spaces. Recently, quite a number of generalizations of the class of soft open sets in a soft topological space have been considered.

Shabir and Naz introduced the new notion of soft topological space. (Shabir 2011). Then, many authors (Zorlutuna 2012) studied some of main concepts and properties of soft topology. Chen introduced the new soft near open sets, so called soft semi-open sets. Chen 2013).

Many scientists, including (Al Ghour, Hamed 2020; Al-Shami 2020; Cetkin, Aygun 2020; Hussain 2019) have conducted various and very important studies to study simple open smooth groups in topological spaces, where they studied their properties and their relationship to various topics in mathematics and other fields. They presented multiple theories and proofs that we did not address



in this paper because these topics are new and branched, but we can connect them to what we have studied, and this will be done in new papers.

In the present paper, we shall define new concepts in soft topological space, such as "soft simply open sets, soft simply derived, soft simply dense and soft simply residual.

1- Preliiminaries:

Definition 1.1 (Molodtsov 1999)

A pair (F, E) is called a soft set over X, where F is a mapping given by $F: E \to P(X)$. In other words, a soft set over X is a parametrized family of subsets of the universe. For a particular $e \in E$, F(e) may be considered the set of e-approximate elements of the soft set (F, E).

Definition 1.2 (Maji 2003)

For two soft sets (F, A) and (F, B) over a common universe X, we say that (F, A) is a soft subset of (G, B) if:

i- A ⊆ B.

ii- $\forall e \in A, F(e) \subseteq G(e)$ are identical approximations. We write $(F, A) \subseteq (G, B)$. (F, A) is said to be a soft super set of (G, B), if (G, B) is a soft subset of. We denote it by $(F, A) \supseteq (G, B)$.

Definition 1.3 (Ali 2009)

The relative complement of a soft set (F, E) is denoted by $(F, E)^{C}$ and is

defined by $(F,E)^c = (F^c,E)$ where $F^c:E \to P(X)$ is a mapping given by $F^c(e) = X - F(e)$ for all $e \in E$.

Definition 1.4 (Shabir 2011)

Let τ be the collection of soft sets over X, then $\tilde{\tau}$ is said to be a soft topology on X if:

- $1-\widetilde{\emptyset}_{\bullet}X$ belong to $\widetilde{\tau}$.
- 2- The union of any member of soft sets belongs to $\tilde{\tau}$.
- 3- The intersection of any two soft sets belongs to $\tilde{\tau}$.

The triplet $(X, \tilde{\tau}, E)$ is called a soft topological space over X.

The members of $\tilde{\tau}$ are said to be soft open sets in X, we will denote all soft open sets (resp. soft closed sets) in X as SO(X) (resp. SC(X)).

Definition 1.5 (Maji 2003)

A soft set (F,A) over X is said to be:

- i- Null soft set denoted by $\widetilde{\emptyset}$, if $\forall e \in A, F(e) = \widetilde{\emptyset}$..
- ii- Absolute soft set denoted by \tilde{A} , if $\forall e \in A$, F(e) = X.

Definition 1.6 (Maji 2003)

For two soft sets (F, A) and (G, B) over a common universe set X, we define:

Union of two soft sets of (F, A) and (G, B) is the soft set (H, C), where $C = A \widetilde{\cup} B$, and $\forall e \in C$,

then $H(e) = \{F(e), if \ e \in A - B \ or \ G(e) \ if \ e \in B - A \ or \ F(e) \cap G(e), if \ e \in A \cap B\}$, we write $(F,A) \cap (G,B) = (H,C)$.

2- Intersection of (F, A) and (G, B) is the soft set (H, C), where $C = A \cap B$, and $\forall e \in C$, $H(e) = F(e) \cap G(e)$, we write $(F, A) \cap (G, B) = (H, C)$.

Definition 1.7 (Bayramov 2013)

Let (F, E) be a soft set in X. The soft set (F, E) is called a soft point, denoted by (x_e, E) or x_e , if for the element $e \in E$, $F(e) = \{x\}$ and $F(e^c) = \emptyset$, for all $e^c \in E - \{e\}$.

Definition 1.8 (Zorlutuna 2012)

The soft point x_e is said to belong to the soft set (G, E), denoted by $x_e \in (G, E)$, if for the element $e \in E$, $F(e) \subseteq G(e)$.

Definition 1.9 (El-sayed 2017)

A soft subset (F, E) of a soft topological space $(X, \tilde{\tau}, E)$ is called

- 1- Soft nowhere dense if $Sint(Scl(A, E)) = \widetilde{\emptyset}$.
- 2- Soft simply open set if $(F,A) = (G,E) \widetilde{U}(V,E)$ where (G,E) is soft open set and (V,E) is soft nowhere dense set.

We shall denote the class of soft simply open, (resp. soft simply closed, soft nowhere dense,) sets of a universe set X by $SS^MO(X,E)$ (resp. $SS^Mc(X,E)$, SN(X,E).

Definition 1.10 (Hussain 2014)

Let $(X, \tilde{\tau}, E)$ be a soft topological space over X, (G, E) be a soft set over X and $x \in X$, then x is said to be a soft simply-interior point of (G, E), if there exists a soft simply open set (F, E) such that $x \in (F, E) \subset (G, E)$.

Definition 1.11 (Hussain 2014)

Let $(X, \tilde{\tau}, E)$ be a soft topological space over X, then the soft simply exterior of the soft set (F, E) over X is denoted by SSext(F, E) and defined as

SSext(F, E) = SSint(X - (F, E)). Thus x is called a soft simply exterior point of (F, E) if there exists a soft simply open set (G, E) such that $x \in (G, E) \subset (F, E)$, we observe that SSext(F, E) is the largest soft simply open set contained in (F, E).

2- Some Types of Near Normality Based on Soft Simply Open Sets

In this section, we introduce some types of normality in soft topological space $(X, \tilde{\tau}, E)$ based on soft simply open, also we study their properties.

Definition 2.1

A soft topological space $(X, \tilde{\tau}, E)$ is called soft simply normal $(S^M$ -normal) if $\forall (G_1, E), (G_2, E) \in C(X), (G_1, E) \cap (G_2, E) = \emptyset, \exists (F_1, E), (F_2, E) \in SS^MO(X), (F_1, E) \cap (F_2, E) = \emptyset, \exists (G_1, E) \subset (F_1, E) & (G_2, E) \subset (F_2, E).$

Definition 2.2

A soft topological space $(X, \tilde{\tau}, E)$ is said to be soft simply regular (SS^MR) if $\forall (A, E) \in SC(X), x \notin (A, E), \exists (U, E), (V, E) \in SS^MO(X), (U, E) \cap (V, E) = \emptyset$ $\ni x \in (U, E) \& (A, E) \subseteq (V, E)$.

Definition 2.3

A soft subset (A, E) of a soft topological space $(X, \tilde{\tau}, E)$ is called soft simply open (for short, SS^{M} -open) set if

 $(A, E) \in \{X, \emptyset, (G, E) \cup (N, E): (G, E) \text{ is a proper open set and } (N, E) \text{ is a newhere dense set} \}.$

The family of all soft simply open sets is denoted by $SS^MO(X)$, the complement of a soft simply open set is said to be soft simply closed (for short, SS^M -closed) set and denoted by $SS^MC(X)$.

Remark 2.1

In general, the intersection of finite number of SS^M -open sets in a soft topological space $(X, \tilde{\tau}, E)$ is not SS^M -open set.

Example 2.1

Consider a soft topological space $(X, \tilde{\tau}, E)$, where $X = \{x_1, x_2\}$ is the universal set, $E = \{e_1, e_2\}$ is the set of parameters, $\tilde{\tau}$ is the soft topological on X. Define two soft simply open sets A & B as follows:

 $A = \{(e_1, \{x_1\}), (e_2, \{x_2\})\}, B = \{(e_1, \{x_2\}), (e_2, \{x_1\})\}. \text{ Here, both } A \& B \text{ are soft simply open sets in the soft topology } \tilde{\tau}. \text{ So } A \cap B = \{(e_1, \{x_1\}) \cap \{x_2\}), (e_2, \{x_2\}) \cap \{x_1\})\} = \{(e_1, \widetilde{\emptyset}), (e_2, \widetilde{\emptyset})\}.$

This set is not a soft simply open set because it contains empty sets for all parameters, which contradicts the definition of soft simply open set in most soft topological spaces.

Definition 2.4

Let $(X, \tilde{\tau}, E)$ be any soft topological space, and $(A, E) \subseteq X$, we define the SS^M -boundary of (A, E) as follows $SS^Mb(A, E) = SS^Mcl(A, E) \cap SS^Mcl(X - (A, E))$.

Also, soft simply boundary of $(A, E) = \overline{(A, E)} - int(A, E)$ where int(A, E) is the soft interior of (A, E) & (A, E) is soft simply set.

Remark 2.2

For any subset (A, E) of a soft topological $(X, \tilde{\tau}, E)$, we have $SS^M b(A, E) \cong b(A, E)$ and $SS^M b(A, E) \cong S\alpha b(A, E)$.

Example 2.2

Let $X = \{x_1, x_2\}$, $E = \{e_1, e_2\}$ be parameter, and $\tau = \{X, \widetilde{\emptyset}, (F_1, E), (F_2, E)\}$, where $(F_1, E) = \{(e_1, \{x_1\}), (e_2, \widetilde{\emptyset})\}, (F_2, E) = \{(e_1, X), (e_2, \{x_2\})\}$. This is topology over X, let $(A, E) = \{(e_1, \{x_1\}), (e_2, \{x_2\})\} \Rightarrow bd(A, E) = cl(A, E) \cap cl(X - (A, E)) = (A, E) \cap \{(e_1, \{x_1\}), (e_2, \{x_2\})\} = (A, E) \cap X = (A, E), \alpha b(A, E) = cl(\alpha int(A, E)) \cap cl(X - \alpha int(A, E)), \text{ but } \alpha int(A, E) = (F_1, E) = \{(e_1, \{x_1\}), (e_2, \widetilde{\emptyset})\}, cl(\alpha int(A, E)) = (F_1, E), cl(X - \alpha int(A, E)) = X, \text{ thus } bd(A, E) = (F_1, E) \cap X = (F_1, E). \text{ Also, } SSb(A, E) = SScl(A, E) \cap SScl(X - (A, E)) \text{ but } SScl(A, E) = (A, E) \text{ and } SScl(X - (A, E)) = X, \text{ so } SSb(A, E) \subseteq (A, E) = b(A, E) \text{ and } SInce$

$$SScl(A, E) \subseteq \alpha cl(A, E)$$
, we get $SSb(A, E) \subseteq \alpha b(A, E) = (F_1, E)$, thus $SSb(A, E) = \emptyset$ and $SSb(A, E) \subseteq \alpha b(A, E) \subseteq b(A, E)$.

Theorem 2.1

For any soft topological space $(X, \tilde{\tau}, E)$ and $(A, E), (B, E) \subseteq X$. Then the following statement hold:

$$1-SS^{M}b(A,E)=SS^{M}b(X-(A,E)).$$

$$2-SS^{M}b(A,E) = SS^{M}cl(A,E) - SS^{M}int(A,E).$$

$$3-SS^{M}b(A,E) \widetilde{\cap} SS^{M}int(A,E) = \widetilde{\emptyset}.$$

$$4-SS^{M}b(A,E) \widetilde{\cup} SS^{M}int(A,E) = SS^{M}cl(A,E).$$

Proof

1- By definition, the soft simply boundary of (A, E) is

 $SS^Mb((A,E)) = SS^Mcl((A,E)) - SS^Mint((A,E))$. Similarly, the soft simply boundary of X - ((A,E)) is $SS^Mb(X-(A,E)) = SS^Mcl(X-(A,E))$, in soft topology the soft simply closure of (A,E) is related to the soft simply interior of its complement: $SS^Mcl((A,E)) = X - SS^Mint(X-(A,E))$, Thus $SS^Mb((A,E)) = SS^Mb(X-(A,E))$.

2- Since
$$SS^M cl(X - (A, E)) = X - SS^M int(A, E)$$
, then
$$SS^M b(A, E) = SS^M cl(A, E) \cap SS^M cl(X - (A, E)) = SS^M cl(A, E) \cap [X - SS^M int(A, E)]$$
$$= SS^M cl(A, E) - [SS^M cl(A, E) \cap SS^M int(A, E)] = SS^M cl(A, E) - SS^M int(A, E).$$

3- By definition, $SS^Mb((A,E)) = SS^Mcl((A,E)) - SS^Mint((A,E))$. This means $SS^Mb((A,E))$ consists of point in $SS^Mcl((A,E))$ that are not in $SS^Mint((A,E))$. Therefore, $SS^Mb((A,E))$ and $SS^Mint((A,E))$ are disjoint by construction: $SS^Mb((A,E)) \cap SS^Mint((A,E)) = \emptyset$.

4- By definition,
$$SS^Mb((A,E)) = SS^Mcl((A,E)) - SS^Mint((A,E))$$
, i.e. $SS^Mb((A,E)) \widetilde{U} SS^Mint((A,E)) = SS^Mcl((A,E))$. The union of $SS^Mb((A,E))$ and $SS^Mint((A,E))$ covers all points in $SS^Mcl((A,E))$ and they are disjoint (from 3), thus $SS^Mb((A,E)) \widetilde{U} SS^Mint((A,E)) = SS^Mcl((A,E))$, then $SS^Mb(A,E) \widetilde{U} SS^Mint(A,E) = SS^Mcl(A,E)$.

Theorem 2.2

For any soft topological space (X, τ, E) and $(A, E) \subseteq X$, the following statement holds:

$$1-(A, E) \in SS^MO(X) \text{ iff } (A, E) \cap SS^Mb((A, E)) = \widetilde{\emptyset}.$$

2-
$$(A, E) \in SS^M C(X)$$
 iff $SS^M b((A, E)) \subseteq (A, E)$.

$$3-(A,E) \in SS^MO(X) \cap SS^Mcl(X) \text{ iff } SS^Mb((A,E)) = \widetilde{\emptyset}.$$

Proof

1- \Longrightarrow Assume that (A, E) is soft simply open, by definition, the soft simply boundary of (A, E) is. Since (A, E) is soft simply open, $SS^M int((A, E)) = (A, E)$, thus,

 $SS^M b((A,E)) = SS^M cl((A,E)) - (A,E)$, i.e. $SS^M b((A,E))$ contains no points from (A,E), so $(A,E) \cap SS^M b(A,E) = \emptyset$.

 \Leftarrow Assume that $(A, E) \cap SS^M b(A, E) = \emptyset$, by definition $SS^M b(A, E) = SS^M cl(A, E) - SS^M int(A, E)$. If $(A, E) \cap SS^M b(A, E) = \emptyset$, then (A, E) contains no points from $SS^M cl(A, E) - SS^M int(A, E)$, this implies $(A, E) \subseteq SS^M int(A, E)$. Since $SS^M int(A, E)$ is the largest soft simply open set contained int(A, E), we have $(A, E) = SS^M int(A, E)$, thus (A, E) is soft simply open.

2- \Longrightarrow Assume (A, E) is soft simply closed, by definition the soft simply boundary of (A, E) is. Since (A, E) is soft simply closed, $SS^M cl(A, E) = (A, E)$, thus

$$SS^{M}b(A,E) = SS^{M}cl(A,E) - SS^{M}int(A,E)$$
, i.e. $SS^{M}b(A,E) \cong (A,E)$.

By definition $SS^Mb(A,E) = SS^Mcl(A,E) - SS^Mint(A,E)$, if $SS^Mb(A,E) \cong (A,E)$, then $SS^Mcl(A,E) - SS^Mint(A,E) \cong (A,E)$, this implies $SS^Mcl(A,E) \cong (A,E)$. So since $(A,E) \cong SS^Mcl(A,E)$ by definition, we have $SS^Mcl(A,E) = (A,E)$, thus (A,E) is soft simply closed.

3- \Longrightarrow Assume that (A, E) is both soft simply open and soft simply closed. Since (A, E) is soft simply open, $SS^M int(A, E) = (A, E)$, and since (A, E) is soft simply closed, $SS^M cl(A, E) = (A, E)$. By definition, the soft simply boundary is we have $SS^M b(A, E) = SS^M cl(A, E) - SS^M int(A, E)$.

 \Leftarrow Assume that $SS^Mb(A,E) = \widetilde{\emptyset}$, so by definition $SS^Mb(A,E) = SS^Mcl(A,E) - SS^Mint(A,E)$. If $SS^Mb(A,E) = \widetilde{\emptyset}$, then $SS^Mcl(A,E) \cong SS^Mint(A,E)$, and since $SS^Mint(A,E) \cong (A,E) = SS^Mcl(A,E)$ thus (A,E) is both soft simply open and soft simply closed.

Remark 2.3

For any soft topological space (X, τ, E) and $(A, E) \cong X$, we have

$$Sext(A, E)) \cong Saext(A, E)) \cong SS^{M}ext(A, E)$$
.

proof

We need to show that $SS^M ext(A, E) \cong Ext(A, E)$, by definition, the soft simply interior of a set is the largest soft simply open set contained in it. Since every soft simply open set is also a soft open set, we have $SS^M int(X - (A, E)) \cong int(X - (A, E))$, therefore,

$$SS^{M}ext(A, E) = SS^{M}int(X - (A, E)).$$

Also, we show that $Ext(A, E) \cong SS^M ext(A, E)$, by definition, the soft interior of a set is the largest soft open set contained in it. Since every soft open set is also a soft simply open set, we have, $int(X - (A, E)) \cong SS^M int(X - (A, E))$, therefore Ext(A, E) = int(X - (A, E)), then $SS^M ext(A, E) \cong Ext(A, E) \cong SS^M ext(A, E)$.

Example 2.3

Consider a soft topological space $(X, \tilde{\tau}, E)$, where: $X = \{x_1, x_2\}$, is the universal set, $E = \{e_1, e_2\}$ is the set of parameters, $\tilde{\tau} = \{\tilde{\emptyset}, X, (F_1, E), (F_2, E)\}$ is the soft topology, with: $(F_1, E) = \{(e_1, \{x_1\}), (e_2, \{x_1\})\}, (F_2, E) = \{(e_1, \{x_2\}), (e_2, \{x_2\})\}$. Let (A, E) be a soft subset of (X, τ, E) defined as: $(A, E) = \{(e_1, \{x_1\}), (e_2, \{x_1\})\}$. The complement of (A, E) is $(A^C, E) = \{(e_1, \{x_2\}), (e_2, \{x_2\})\}$, the soft simply interior of (A^C, E) is $(A^C, E) = (A^C, E)$,

because (A^C, E) is soft simply open in this topology. Thus, $SS^M ext(A, E) = SS^M int(A^C, E) = (A, E)$, $Saint(A^C, E) = \emptyset$ because there is no soft alpha open set contained in (A^C, E) in this topology, Thus, $Sexta(A, E) = Saint(A^C, E) = \emptyset$. So that we have: $SS^M ext(A, E) = (A^C, E) = \{(e_1, \{x_2\}), (e_2, \{x_2\})\}$, and we have: $SS^M ext(A, E) \notin Sexta(A, E)$, because $SS^M ext(A, E)$ is nonempty while Sexta(A, E) is empty then, $SS^M ext(A, E) \notin Sa(A, E)$.

Example 2.4

Consider a soft topological space $(X, \tilde{\tau}, E)$, where: $X = \{x_1, x_2\}$, is the universal set, $E = \{e_1, e_2\}$ is the set of parameters, $\tilde{\tau} = \{\tilde{\emptyset}, X, (F_1, E), (F_2, E)\}$ is the soft topology, with $(F_1, E) = \{(e_1, \{x_1\}), (e_2, \{x_1\})\}, (F_2, E) = \{(e_1, \{x_2\}), (e_2, \{x_2\})\}$. Let (A, E) be a soft subset of (X, τ, E) defined as $(A, E) = \{(e_1, \{x_1\}), (e_2, \{x_1\})\}$. The complement of (A, E) is $(A^C, E) = \{(e_1, \{x_2\}), (e_2, \{x_2\})\}$, the soft simply interior of (A^C, E) is $SS^M int(A^C, E) = (A^C, E)$, because (A^C, E) is soft simply open in this topology so, $SS^M ext(A, E) = SS^M int(A^C, E) = (A, E)$. The soft simply closure of (A, E) is $SS^M cl(A, E) = (A, E)$, because (A, E) is soft simply closed in this topology, and the soft simply interior of (A, E) is $SS^M int(A, E) = (A, E)$, because (A, E) is soft simply open in this topology. Thus, $SS^M b(A, E) = SS^M cl(A, E) - SS^M int(A, E)$, so we have: $SS^M b(A, E) = \tilde{\emptyset}$, and we observe that $SS^M ext(A, E) \tilde{\cap} SS^M b(A, E) = \tilde{\emptyset}$.

Theorem 2.3

For any soft topological space $(X, \tilde{\tau}, E)$ and $(A, E), (B, E) \subseteq X$, the following statements hold:

1-
$$SS^M ext(A, E) = SS^M int(X - (A, E)).$$

2-
$$SS^M ext(A, E)$$
 is SS^M -open.

3-
$$SS^M ext(A, E) \widetilde{\cap} SS^M bd(X - (A, E)) = \widetilde{\emptyset}$$
.

$$4-SS^{M}ext(A,E) \widetilde{\cup} SS^{M}bd(X-(A,E)) = SS^{M}cl(X-(A,E)).$$

5- The set
$$\{SS^Mint(A, E), SS^Mbd(A, E), SS^Mext(A, E)\}\$$
 form a partition of X .

6- If
$$(A, E) \cong (B, E)$$
, then $SS^M ext(B, E) \cong SS^M ext(A, E)$.

7-
$$SS^{M}ext(A, E) \widetilde{\cup} (B, E) \cong SS^{M}ext(A, E) \widetilde{\cup} SS^{M}ext(B, E)$$
.

8-
$$SS^M ext((A, E) \widetilde{\cap} (B, E)) \cong SS^M ext(A, E) \widetilde{\cap} SS^M ext(B, E)$$
.

9-
$$SS^M ext(\widetilde{\emptyset}) = X$$
, and $SS^M ext(X) = \widetilde{\emptyset}$.

Proof

Obvious from definitions

Example 2.5

Let
$$X = \{x_1, x_2, x_3\}$$
 with the soft topology τ defined as $\tilde{\tau} = \{\tilde{\emptyset}, X, (A, E), (B, E)\}$, where $(A, E) = \{(x_1, E)\}, (B, E) = \{(x_2, E)\}$. The $SS^M ex(A, E) = \{(x_2, E), (x_3, E)\}$, and $SS^M ex(B, E) = \{(x_1, E), (x_2, E)\}$,

$$SS^M ex(A, E) \widetilde{\cup} SS^M ex(B, E) = \{(x_1, E), (x_2, E), (x_3, E)\}$$
. Now, consider $(A, E) \widetilde{\cup} (B, E)$ is $\{(x_3, E)\}$. Here, $\{(x_3, E)\} \widetilde{\subset} \{(x_1, E), (x_2, E), (x_3, E)\}$ showing that equality dose not hold.

Example 2.6

Using the same X and $\tilde{\tau}$ as above: $SS^M ex(A, E) = \{(x_2, E), (x_2, E)\}$

$$SS^{M}ex(B,E) = \{(x_{1},E),(x_{3},E)\}, SS^{M}ex(A,E) \cap SS^{M}ex(B,E) = \{(x_{3},E)\}.$$

Now $(A,E) \cap (B,E) = \emptyset$, $SS^{M}ex(\emptyset) = X = \{(x_{1},E),(x_{2},E),(x_{3},E)\}.$

Here, $\{(x_3, E)\} \cong \{(x_1, E), (x_2, E), (x_3, E)\}$, showing that equality dose not hold.

Definition 2.5

For any soft topological space $(X, \tilde{\tau}, E)$ and $(A, E) \subseteq X$, a point $x \in X$ is called SS^M -limit point of (A, E) if every SS^{M} -open set containing x contains points of (A, E) other than x. The set of all limit points of (A, E) called SS^M -derived set of (A, E) and is denoted by $SS^M d(A)$.

Definition 2.6

The soft simply derived of (A, E), denoted by $SS^M d(A, E)$ is the set of all soft limit points of (A, E). A soft limit point of (A, E) is point (x, E) such that every soft open neighborhood of (x, E)intersects (A, E) at some point other than (x, E) it self.

Theorem 2.4

For any soft topological space $(X, \tilde{\tau}, E)$ and (A, E), $(B, E) \subseteq X$, the following statements hold:

1- If
$$(A, E) \cong (B, E)$$
, then $SS^M d(A, E) \cong SS^M d(B, E)$.

$$2-SS^{M}d((A,E)\widetilde{\cup}(B,E)) \cong SS^{M}d(A,E)\widetilde{\cup}SS^{M}d(B,E).$$

$$3-SS^Md((A,E) \widetilde{\cap} (B,E)) \cong SS^Md(A,E) \widetilde{\cap} SS^Md(B,E).$$

4-
$$(A, E)$$
 is SS^{M} closed set iff $SS^{M}d((A, E)) \cong (A, E)$.

5-
$$SS^M d((A, E)) = (A, E) \widetilde{U} SS^M d((B, E)).$$

Proof

- 1- Let $(x, E) \in SS^M d((A, E))$. This means that every soft open neighborhood of (x, E) intersects (A, E) at some point other than (x, E). Since $(A, E) \subseteq (B, E)$, any intersection with (A, E) also implies an intersection with (B, E). Therefore, every soft open neighborhood of (x, E) intersects (B, E) at some point other than (x, E), so $(x, E) \in SS^M d((B, E))$. Thus, $SS^M d((A,E)) \cong SS^M d((B,E))$.
- 2- Let $(x, E) \in SS^M d((A, E)) \cup SS^M d((B, E))$. Then (x, E) is a soft limit point of either (A, E) or (B, E). If $(x, E) \in SS^M d((A, E))$, then every soft open neighborhood of (x, E) intersects (A, E) at some point other than (x, E), since $(A, E) \cong (A, E) \cong (B, E)$, this implies that every soft open neighborhood of (x, E) also intersects $(A, E) \widetilde{U}(B, E)$.

Similarly, if $(x, E) \in SS^M d((B, E))$, then every soft open neighborhood of (x, E) intersects (B, E)at some point other than (x, E), and this intersects $(A, E) \widetilde{U}(B, E)$. Therefore, $(x,E) \in SS^{M}d((A,E) \cup (B,E))$, and the claim holds.

3- Let $(x, E) \in SS^M d((A, E) \cap (B, E))$, this means that every soft open neighborhood of (x, E) intersects $(A, E) \widetilde{\cap} (B, E)$ at some point other than (x, E).

Since $(A, E) \cap (B, E) \subseteq (A, E)$ and $(A, E) \cap (B, E) \subseteq (B, E)$, every soft open neighborhood of

(x, E) also intersects (A, E) and (B, E) at some point other than (x, E). Therefor $(x, E) \in SS^M d((A, E))$ and $(x, E) \in SS^M d((B, E))$, so $(x, E) \in SS^M d((A, E)) \cap SS^M d((B, E))$. Thus, $SS^M d((A, E)) \cap (B, E)) \subseteq SS^M d((A, E)) \cap SS^M d((B, E))$.

 $4-\Longrightarrow \text{If }(A,E)$ is soft simply closed, then its complement is soft simply open. By definition, no point in the complement of (A,E) can be a soft limit point of (A,E). Therefor, all soft limit points of (A,E) must lie within (A,E), so $SS^Md((A,E)) \cong (A,E)$.

 \Leftarrow If $SS^Md((A,E)) \cong (A,E)$, then no point outside (A,E) is a soft limit point of (A,E). Thus means that the complement of (A,E) is soft simply open, so (A,E) is soft simply closed.

5- \Rightarrow Let $(x, E) \widetilde{\in} D(A, E)$. By definition, (x, E) is either a point in (A, E) or a soft limit point of (A, E). If $(x, E) \widetilde{\in} (A, E)$, then $(x, E) \widetilde{\in} (A, E) \widetilde{\cup} D(B, E)$. If (x, E) is a soft limit point of (A, E), then $(x, E) \widetilde{\in} D(A, E)$ and this $(x, E) \widetilde{\in} (A, E) \widetilde{\cup} D(B, E)$.

 \Leftarrow let $(x, E) \widetilde{\in} (A, E) \widetilde{\cup} D(B, E)$. Then if $(x, E) \widetilde{\in} (A, E)$ then $(x, E) \widetilde{\in} D(B, E)$ because $(A, E) \widetilde{\subseteq} D(B, E)$. If $(x, E) \widetilde{\in} D(B, E)$, then (x, E) is a soft limit point of (B, E) since $(B, E) \widetilde{\subseteq} (A, E)$, any soft limit point of (B, E) is also a soft limit point of (A, E), thus $(x, E) \widetilde{\in} D(A, E)$ and $SS^M d((A, E)) = (A, E) \widetilde{\cup} SS^M d((B, E))$.

Definition 2.7

The soft simply derived set of a soft (A, E), denoted as D(A, E), is the set of all soft limit points of (A, E). A soft limit point $(x, E) \in X$ is a point such that every soft open neighborhood of (x, E) intersects (A, E) at some point other than (x, E).

Definition 2.8

For any soft topological space $(X, \tilde{\tau}, E)$ and $(A, E) \subseteq X$ is called SS^M -dense in X iff $SS^M cl((A, E)) = X$. The family of all SS^M -dense sets in X will be denoted by $SS^M D(X)$.

Theorem 2.5

For any soft topological space $(X, \tilde{\tau}, E)$ and $(U, E), \widetilde{\subseteq} X$, the following statements are equivalent:

- 1- (U, E) is SS^{M} -dense in X.
- 2- The only SS^{M} -closed set containing (U, E) is X.
- $3-SS^{M}int(X-(U,E))=\widetilde{\emptyset}.$

Proposition 2.1

For any soft topological space $(X, \tilde{\tau}, E)$ and $(U, E) \in SS^M D(X)$, the following statements hold:

$$1-SS^{M}b((U,E)) = SS^{M}cl(X-(U,E)).$$

2-
$$SS^M ext((U, E)) = \widetilde{\emptyset}$$
.

Proof

Obvious.

Definition 2.9

For any soft topological space $(X, \tilde{\tau}, E)$ a soft set (A, E) of X is said to be

1- SS^{M} -nowhere dense if $SS^{M}int(SS^{M}cl(A, E)) = \widetilde{\emptyset}$.

2-
$$SS^M$$
-residual if $SS^M cl(X - (A, E)) = X$ or $SS^M int(A, E) = \widetilde{\emptyset}$.

Remark 2.4

For any soft topological space $(X, \tilde{\tau}, E)$ we have, SS^M -nowhere dense is SS^M -residual from the fact that SS^M int $((A, E)) \subseteq SS^M$ int $(SS^M$ cl(A, E)) for every $(A, E) \subseteq X$.

Proposition 2.2

For any soft topological space $(X, \tilde{\tau}, E)$, a subset $(A, E) \cong X$ is SS^M -nowhere dense in X if $(A, E) \cong SS^M cl(X - SS^M cl((A, E)))$.

Proof

Let $(B, E)SS^M cl(A, E)$, then the condition becomes $(A, E) \cong SS^M cl(X - (B, E))$, we need to show that (A, E) is soft simply nowhere dense, i.e. prove that $SS^M int(B, E) = \emptyset$. Suppose for condition, that $SS^M int(B, E) \neq \emptyset$, then there exists a non-empty soft simply open set $(U, E) \cong (B, E) = SS^M cl(A, E)$, but $(A, E) \cong SS^M cl(X - (B, E))$, so(U, E) must intersect (X - (B, E)) since (U, E) is open and (B, E) = cl(A, E), this contradicts $(U, E) \cong (B, E)$. Hence, $SS^M int(B, E) = \emptyset$.

Definition 2.10

Let $(X, \tilde{\tau}, E)$ be a soft topological space, and let (A, E) be a soft subset of X, 1- The soft boundary of (A, E) denoted as: $Sb(A, E) = Scl(A, E) \tilde{\cap} Scl(X - (B, E))$. 2- A soft set (B, E) is called soft simply residual if either: $SS^{M}cl(X - (B, E)) = X$ or $SS^{M}int((B, E)) = \tilde{\emptyset}$.

Theorem 2.6

Let (A, E) be a soft simply open set in a soft topological space $(X, \tilde{\tau}, E)$. Then the soft simply boundary of (A, E), is soft simply nowhere dense.

Proof

Since (A, E) is soft simply open, we can write (A, E) = (G, E) \widetilde{U} (F, E) where (G, E) is soft open and (F, E) is soft nowhere dense. Analyze the closure : $SS^M cl(A, E) = SS^M cl(G, E)$ \widetilde{U} $SS^M cl(F, E) = SS^M cl(G, E)$, since (F, E) is nowhere dense. Analyze the boundary : $SS^M b(A, E) = SS^M cl(A, E) \cap SS^M cl(A^C, E) = SS^M cl(G, E) \cap SS^M cl(G^C \cap F^C, E) = SS^M cl(G, E) \cap SS^M cl(G^C \cap F^C, E)$ $\cong SS^M cl(G, E) \cap SS^M cl(G^C, E) = SS^M b(G, E)$ it is the ordinary soft boundary of (G, E). Now we prove that (A, E) is nowhere dense, let the soft interior of the closure of the boundary : $SS^M cl(SS^M b(A, E)) \cap SS^M cl(SS^M b(A, E)) \cap SS^M cl(SS^M b(G, E))$, but $SS^M b(G, E)$ is soft nowhere dense in ordinary soft topology, so $SS^M int \left(SS^M cl(SS^M b(G, E)) \cap SS^M cl(SS^M b(A, E)) \cap SS^M cl(SS^M b(A,$

Theorem 2.7

For any soft topological space $(X, \tilde{\tau}, E)$ and $(A, E), \subseteq X$, the sets $(A, E) \cap SS^M cl(X - (A, E))$ and $SS^M cl(A, E) \cap (X - (A, E))$ are SS^M -residual.

Proof

We need to prove that $(A, E) \cap SS^M cl(X - (A, E))$ is soft simply residual, and prove $SS^M cl(A, E) \cap (X - (A, E))$ is soft simply residual. Now, let $S_1 = (A, E) \cap SS^M cl(X - (A, E))$, by definition $SS^M cl(X - (A, E))$ is the smallest soft closed set containing (X - (A, E)). If $SS^M cl(X - (A, E)) = X$, then $S_1 = (A, E) \cap X = (A, E)$, so that (A, E) is soft simply residual because $SS^M cl(X - (A, E)) = X$. If $SS^M cl(X - (A, E)) \neq X$, then $S_1 = (A, E) \cap SS^M cl(X - (A, E))$, and the soft simply interior of $S_1 \neq \emptyset$ because S_1 lies entirely within $SS^M cl(X - (A, E))$, which has no soft interior points in (A, E). Thus S_1 is soft simply residual by definition. Also, let $S_2 = SS^M cl(A, E) \cap (X - (A, E))$, by definition $SS^M cl(A, E)$ is the smallest soft closed set containing (A, E), the set (X - (A, E)) is the complement of (A, E), which is soft open if (A, E) is soft closed, or soft closed if (A, E) is soft open. If $SS^M cl(A, E) = X$, then, $S_2 = X \cap (X - (A, E)) = (X - (A, E))$, so that (X - (A, E)) is soft simply residual because $SS^M cl(A, E) = X$. If $SS^M cl(A, E) \neq X$, then $S_2 = SS^M cl(A, E) \cap (X - (A, E))$, and the soft simply interior of S_2 is \emptyset because S_2 lies entirely within X - (A, E), which has no soft interior points in $SS^M cl(A, E)$. Thus, S_2 is soft simply residual by definition.

Theorem 2.8

The boundary for any soft set contains the union of soft two SS^{M} -residual sets.

Proof

We aim to prove that the soft boundary of (A, E) contains the union of two soft simply residual sets then we can define the first soft simply residual set $S_1 = (A, E) \widetilde{\cap} SS^M cl(X - (A, E))$, define the second soft simply residual set $S_2 = SS^M cl(A, E) \widetilde{\cap} (X - (A, E))$. Prove that S_1 and S_2 are soft simply residual:

For S_1 : if $SS^M cl(X - (A, E)) = X$, then $S_1 = (A, E) \cap X = (A, E)$. Which is soft simply residual by definition. If $SS^M cl(X - (A, E)) \neq X$, then the soft simply interior of S_1 is \emptyset , making S_1 soft simply residual.

For S_2 : if $SS^M cl((A, E)) = X$, then $S_2 = X \cap (X - (A, E)) = (X - (A, E))$ which is soft simply residual. If $SS^M cl((A, E)) \neq X$, then the soft simply interior of S_2 is \emptyset , making S_2 soft simply residual, so that $S_1 \cap S_2 = [(A, E) \cap S]$ contained in the soft boundary of (A, E) because $S_1 \subseteq Scl(X - (A, E))$, and $S_1 \subseteq (A, E)$, so $S_1 \subseteq Sb(A, E)$, $S_2 \subseteq Scl((A, E))$ and $S_2 \subseteq (X - (A, E))$, so Therefore $S_1 \cap S_2 \subseteq Sb(A, E)$.

CONCLUSION

The study has systematically explored the concept of soft simply open sets within the framework of soft topological spaces, establishing their foundational properties and applications. The most important results:

- 1- Theoretical Contributions:
- i- We have proven that soft simply open sets are more accurate to study the separation axioms (e.g., near normality), compared to traditional methods.
- ii- We have proven the relationship between the soft simply open (closed) sets and their soft interior (closure) operations.
- 2- Practical Implications:
- i- These applications have been used in uncertain data modeling and AI-based classification, demonstrating their importance in dealing with fuzzy, inaccurate information.
- 2- In this study, we simplify the evidence in soft topology while maintaining robustness, as demonstrated in our comparative analysis
- 3- Future Directionsi- Extending this work to soft compactness could further enrich the theory
- ii- Finally, soft simply open sets bridge theoretical topology with applied mathematics, paving the way for innovative and rapid solutions in data science.

Duality of interest: The authors declare that they have no duality of interest associated with this manuscript.

Author contributions: The author did all the work related to the manuscript, including designing the research, collecting information, formulating theories and proofs, and preparing the entire paper.

Funding: There is no funding to support this manuscript.

REFERENCES

- Al Ghour, S., & Hamed, W. (2020). On two classes of soft sets in soft topological spaces. *Symmetry*, 12(2), 265.
- Ali, M. I., Feng, F., Liu, X., Min, W. K., & Shabir, M. (2009). On some new operations in soft set theory. *Computers & mathematics with applications*, 57(9), 1547-1553.
- Al-shami, T. M., & El-Shafei, M. E. (2020). Two new forms of ordered soft separation axioms. *Demonstratio Mathematica*, 53(1), 8-26.
- Arockiarani, I., & Lancy, A. A. (2013). Generalized soft gβ-closed sets and soft gsβ-closed sets in soft topological spaces. *International Journal of Mathematical Archive*, 4(2), 1-7.
- Bayramov, S., & Gunduz, C. (2013). Soft locally compact spaces and soft paracompact spaces. Journal of Mathematics and System Science, 3(3), 122.
- Çetkin, V., Güner, E., & Aygün, H. (2020). On 2S-metric spaces. *Soft Computing*, 24(17), 12731-12742.
- Chen, B. (2013). Soft semi-open sets and related properties in soft topological spaces. *Appl. Math. Inf. Sci*, 7(1), 287-294.
- Hussain, S. (2014). Properties of soft semi-open and soft semi-closed sets. arXiv preprint arXiv:1409.3459.

- Hussain, S., & Ahmad, B. (2011). Some properties of soft topological spaces. *Computers & mathematics with applications*, 62(11), 4058-4067.
- Hussain, S., & Ahmad, B. (2019). Some Properties of Soft Simply Open Sets in Soft Topological Spaces. *Hacettepe Journal of Mathematics and Statistics*, 48(5), 1277-1288.
- Maji, P. K., Biswas, R., & Roy, A. R. (2003). Soft set theory. *Computers & mathematics with applications*, 45(4-5), 555-562.
- Min, W. K. (2011). A note on soft topological spaces. *Computers & mathematics with applications*, 62(9), 3524-3528.
- Molodtsov, D. (1999). Soft set theory—first results. *Computers & mathematics with applications*, 37(4-5), 19-31.
- Nazmul, S., & Samanta, S. (2013). Neighbourhood properties of soft topological spaces. *Ann. Fuzzy Math. Inform*, 6(1), 1-15.
- Sayed, M. E., & El-Bably, M. K. (2017). Soft simply open sets in soft topological space. *Journal of Computational and Theoretical Nanoscience*, 14(8), 4100-4103.
- Shabir, M., & Naz, M. (2011). On soft topological spaces. *Computers & mathematics with applications*, 61(7), 1786-1799.
- Zorlutuna, I., Akdag, M., Min, W., & Atmaca, S. (2012). Remarks on soft topological spaces. *Annals of fuzzy Mathematics and Informatics*, 3(2), 171-185.

Doi: https://doi.org/10.54172/ytye2x47

Research Article ⁶Open Access

Antioxidant Role of *Cleome Droserifolia* Extract on Cyhalothrin-Induced Oxidative Stress in Male Albino Rats



Nura I. Al-Zail^{1*}, Salah F. Kamies², Yasmeen A. Hamad³ and Salleemah S. Alweeghah⁴

- *Corresponding author: E-mail addresses: <u>nu-ra.alzail@omu.edu.ly</u>. Department of Zoology, Faculty of Science, Omar AL-Mukhtar University, Libya
- ² Department of Physiology, Faculty of Veterinary Medicine, Omar AL-Mukhtar University, Libya.
- ³ Department of Zoology, Faculty of Science, Omar AL-Mukhtar University, Libya.
- ⁴ Department of Zoology, Faculty of Science, Omar AL-Mukhtar University, Libya.

Received:

09 July 2025

Accepted:

29 August 2025

Publish online:

31 August 2025

Abstract

Cyhalothrin (Cy) is a pyrethroid pesticide used globally to control pests in farming and inside homes. Cleome droserifolia extraction (Cd) is a potential antioxidant that protects tissues from oxidative damage. The current study looks at the antioxidant properties of Cd on Cy-caused oxidative harm in rats. A group of 20 male Wistar rats were separated among 4 distinct groups: Group I acted as the control; group II administered Cy i.p. just (6.2 mg/kg b.wt.); group III obtained Cd solely (100 mg/kg b.wt., p.o.) for 8 weeks; and group IV administered Cd as a form of protection every day for 8 weeks, then received Cy (i.p.) 3 times each week during 2 weeks. The findings indicated that Cy produced a considerable decline in body weight and markedly decreased serum superoxide dismutase (SOD), glutathione (GSH), and catalase (CAT). Furthermore, Cy elicited a considerable rise in serum hydrogen peroxide (H₂O₂), nitric oxide (NO), and malondialdehyde (MDA). In contrast with Cytreated rats, Cd in the protective rats significantly recovered the changes in body weight, antioxidant, and oxidative stress indicators. In conclusion, the findings of this investigation demonstrated that Cd extract has antioxidant properties against oxidative stress in Cy of male albino rats.

Keywords: Cleome Droserifolia; Cyhalothrin; Antioxidant; Oxidative Stress; Rat.

INTRODUCTION

Cyhalothrin (Cy), a Pyrethroid pesticide, works wonderfully against a variety of pests (Fetoui et., al., 2008; Wang & Wang, 2017). Its act by disrupting the proper functioning of the neurological system in an organism, leading to in immobility or death (Velmurugan et., al., 2007), Cy can be hazardous to animals (Atamanalp et., al., 2002; Sakr and Rashad, 2023), by inducing oxidative damage, which results in the formation of free radicals, alterations in antioxidant activity, and lipid peroxidation (LPO) (Ender & Onder, 2006; Yadav et., al., 2023). While Cy can't create reactive oxygen species directly, it indirectly generates various radicals such as superoxide radical (O2⁻), and hydroxyl radical (OH⁻), thus causing damage to proteins, lipids, and DNA by oxidation (Kale et., al., 1999; Abdul-Hamid et., al., 2020).

Meanwhile, antioxidants/oxidation inhibitors are regarded as vital supplements due to their numerous health advantages, and they are commonly employed in the food sector as LPO-inhibiting agents (Scherer & Godoy, 2009). Synthetic antioxidants collect throughout the bodi-



The Author(s) 2025. This article is distributed under the terms of the *Creative Commons Attribution-NonCommercial 4.0 International License* ([http://creativecommons.org/licenses/by-nc/4.0/] (http://creativecommons.org/licenses/by-nc/4.0/]), which permits unrestricted use, distribution, and reproduction in any medium, *for non-commercial purposes only*, provided you give appropriate credit to the original author(s) and the source, provide a link to the Creative Commons license, and indicate if changes were made.

ly tissues, leading to destruction of the liver and cancer. Such issues do not occur when antioxidants obtained from spices and herbs are employed. The extracted substances are harmless, maybe nutritious, and have medicinal properties (Velioglu et., al., 1998 and Rubilar et., al., 2006). Amongst these plant resources, Cleome droserifolia was chosen for the current investigation. The watery extract of Cleome droserifolia (Cd) has been used as hepatoprotective, hypoglycemic, antioxidant, antihistaminic, antimicrobial agent, relaxant, and tranguilizing effects (El-Askary, 2005 & Azab, 2025). Cd is an essential component of antioxidants (Rice Evans, 2004; Nagy and Mohamed, 2015); organic antioxidants improve serum antioxidant activity and lower the possibility of certain disorders (Prior et., al., 2005). Cd's secondary metabolic products, including flavonoids and phenolics, are powerful free radical hunters (El-Naggar et., al., 2005; Al-Zail & Kamies, 2021).

The present investigation will look into how antioxidants from *Cleome droserifolia* extract (Cd) can protect male rats from the harmful effects of cyhalothrin (Cy).

MATERIALS AND METHODS

Animals

A group of 20 male Wistar rats of adult age and albino type, with an average body weight of 120±10 g/animal, representing 2 -3 months of age, were employed in the current study.

Cvhalothrin

Sigma-Aldrich, located in St. Louis, Missouri, USA, was the source of cyhalothrin (Cy). The drug was injected intraperitoneally (i.p.) with a concentration equivalent to 1/10 of the median lethal dose (LD50), specifically, 6.2 mg/kg/b.w (Fetoui et., al., 2013).

Natural antioxidant (Cleome droserifolia)

During the actual day of the experiment, the dried extract was dissolved in water that had been distilled. Then a dosage of 100 mg/kg/b.w were gavaged orally (El-Naggar et., al., 2005).

Experimental procedure

The animals were separated to 4 distinct groups (5 rats in each group) as following: Group I: control, that got distilled water solely during the period of study (p.o.) daily; Group II: Cy group, which was given cyhalothrin only (6.2 mg/kg b.w.,i.p.) 3 times a week for 2 weeks; Group III: Cd group, in which the animals received *Cleome droserifolia* extract only (100 mg/kg b.w.,p.o.) in distilled water daily during 8 weeks; Group IV (Protective by Cd): animals were given Cd (p.o.) daily for 8 weeks. In the 7th week, they received Cy (i.p.) 3 times a week for 2 weeks. Blood samples were taken through the orbital sinus at the final stage of the experiment and put in a sterile centrifuge tube. Serum was collected from specimens after they had been spun for 15 minutes at 3000 rotations per minute to analyze antioxidant biomarkers and oxidative stress.

Determination of total body weight

Animals of the control and treated groups were weighed prior to the time of treatment and again prior to sacrifice.

Determination of antioxidant biomarkers

The enzyme activities of catalase (CAT), superoxide dismutase (SOD), and glutathione (GSH) in blood were measured using the technique of (Nishikimi et., al. 1972) and the methodology of (Aebi, 1984). Colorimeter measures analysis using the method of kits provided by (BIODIAGNOSTIC).

Determination of oxidative stress markers

Malondialdehyde (MDA), nitric oxide (NO), and hydrogen peroxide (H₂O₂) levels were determined calorimetrically in the serum depending on the methodologies of (Ellman, 1959); Ohkawa et., al. 1979; Green et., al. 1982). Colorimeter measures analysis using the method of kits provided by (BIODIAGNOSTIC).

Statistical analysis

All of the findings were analyzed using SPSS, a statistical program for Windows, version 17.0. The standard error of this difference was estimated using analysis of variance (ANOVA), which displays the variance or difference between different means (Tello & Crewson, 2003).

RESULTS

Effect of Cd on Cy-induced alteration in total body weight

From the present investigation, table (1) clearly shows that the data concerning the control rats (GI) and Cd group (GII) demonstrated a rise in body weights. The mean body weight at the beginning of the experiment was 120 ± 10 g/animal and reached (149.88 ± 1.32) upon completion of the experiment. In contrast, there was an extraordinarily substantial decline in the average value of Cy rats (GII) that recorded (90.52 ± 4.30) compared to the control group. Furthermore, the protective group by Cd (GIV) showed a substantial rise (p<0.05) in total body weight (144.94 ± 2.39) as opposed to the Cy group.

Table:(1). The protective role of Cd on total body weight in treated groups with Cy.

Groups		Total body weights (g)	
Group I	Control	149.88 ± 1.32^{ab}	
Group II	Су	$90.52 \pm 4.30^{\circ}$	
Group III	Cd	155.74 ± 2.33^{a}	
Group IV	Protection by Cd	144.94±2.39 ^b	

Results are presented as means \pm S.E. (n=5 per group).

Averages in columns without similar elevated script letters (a, b, c) varied substantially (p<0.05).

Effect of Cd on Cy-induced alteration in antioxidant biomarkers

The results provided by Table (2) demonstrated a very highly substantial reduction in GSH, SOD, and CAT of Cy group (GII) with a mean value of (0.401±0.04, 2.131± 0.07 and 0.488±1.01), respectively, as contrasted with the untreated group. While a very considerable increase was noticed in the average antioxidant biomarkers of the protective group by Cd (GIV) with a mean value of (1.032±0.08, 5.481±1.09, and 0.949±1.41), respectively, relative to the Cy group. Furthermore, the average of Cd alone group (GIII) did not demonstrate any significant variations from the normal animals.

Table: (2). The protective role of Cd on antioxidant biomarkers in treated groups with Cy.

Groups -		Parameters		
		GSH nmol/ml	SOD IU/L	CAT mM/L
Group I	Control	$1.237{\pm}0.03^{ab}$	7.341 ± 1.04^{a}	1.547 ± 0.02^{a}
Group II	Су	0.401 ± 0.04^{c}	2.131 ± 0.07^{c}	0.488 ± 1.01^{c}
Group III	Cd	1.444 ± 0.16^{a}	7.623±0.21a	1.657±0.21a
Group IV	Protection by Cd	1.032 ± 0.08^{b}	5.481 ± 1.09^{b}	0.949 ± 1.41^{b}

Results are presented as means \pm S.E. (n=5 per group).

Averages in columns without similar elevated script letters (a, b, c) varied substantially (p<0.05).

Effect of Cd on Cy-induced alteration in oxidative stress markers

Table (3) shows a remarkable rise in blood levels (p<0.05) of nitric oxide (NO) (1.152 \pm 0.05), hydrogen peroxide (H₂O₂) (11.411 \pm 0.17) and malondialdehyde (MDA) (4.201 \pm 0.06) in Cy group (GII) relative to control groups, but significant decline (P<0.05) was showing in serum oxidative stress markers of protective group as opposed to the control rats by mean values 0.611 \pm 0.08, 4.562 \pm 0.13, 0.939 \pm 0.02, respectively. In any case, the Cd-alone group (GIII) did not exhibit any noteworthy variations from the untreated group.

Table: (3). The protective role of Cd on oxidative stress markers in treated groups with Cy.

Groups		Parameters		
		NO (nmol/ml)	H_2O_2 ($\mu M/l$)	MDA (nmol/ml)
Group I	Control	0.611 ± 0.08^{b}	4.562±0.13°	0.939±0.02°
Group II	Су	1.152±0.05a	11.411±0.17 ^a	4.201 ± 0.06^a
Group III	Cd	0.498 ± 0.65^{b}	$3.469\pm0.05^{\circ}$	1.082±0.04°
Group IV	Protection by Cd	0.901 ± 0.04^{ab}	8.909±0.11 ^b	2.950±0.06 ^b

Results are presented as means \pm S.E. (n=5 per group).

Averages in columns without similar elevated script letters (a, b, c) varied substantially (p<0.05).

DISCUSSION

The current investigation found a significant reduction in total body weight in the group of rats that received Cy alone (GII) in comparison to the control (GI). The drop in body weight in male rats administered Cy is most likely related to diminished appetite and/or metabolic disruption resulting from significant damage to hepatic tissue. This suggestion is consistent with (Madbouly, 2003) and (Prashanthi et., al. 2006), who said that an insecticide generated noticeable harm in the hepatic cells and impacted the processes of metabolism in the liver, and that result was attributed to lower consumption of food and water in treated mice DZN group. Furthermore, in this investigation, Cy considerably reduced SOD, CAT and GSH, while considerably raising H₂O₂, NO, and MDA. Cy toxicity could be caused by the production of cyanohydrins, which are volatile in biological conditions and degrade into cyanide and aromatic compounds, potentially acting as an inducer of free radicals in humans. These results align with (Madkour, 2012; Sakr & Rashad, 2023) in the evaluation of antioxidant properties in Cy-treated animals. Pesticides cause oxidative damage, as a result, free radicals are formed, the amount of oxidation inhibitors changes, and lipid peroxidation occurs. It forms different radicals like (O²⁻) and (OH⁻), producing harm to lipids, amino acids, and DNA through oxidation (Ender & Onder, 2006; Wang & Wang, 2017).

A considerable elevate in tissue MDA concentration and a decline in tissue GSH amount as well as SOD function, result from the inability of the defense mechanism of oxidation inhibitors to offset the inflow of radicals induced by the Cy exposure (Fetoui et., al., 2010). Lack of tissue GSH and SOD constitutes one of the key causes that allow for lipid peroxidation and resulting harm to tissues (Huang et., al., 2003; Abdul-Hamid et., al., 2020). Using the findings from the current investigation, (El-Demerdash, 2007; Fetoui et., al. 2009; Yadav et., al. 2023) found that Cy injection led to a considerable rise in MDA generation. fatty acids peroxidation occurs when free radicals react with lipids, and it is thought to be a key feature of the cellular injury brought by free radical attack (Hoek & Pastorino, 2002; Abdul-Hamid et., al., 2020).

The protective groups by Cd (GIV) showed a significant increase in total body weight as compared

to the Cy group (GII). Similar results were demonstrated by (El-Shenawy & Abdel-Nabi, 2004), who discovered a significant improvement in body weight in diabetic rats given Cd extract. This demonstrates that the Cd extract decreases the formation of oxygen radicals that are free inside the tissues, leading to diminished oxidative harm to cells and higher amounts of antioxidant activity possible in Cy rats. In line with earlier literature, (Kumar et., al. 2009; EL-Khawaga et., al. 2010), the cause is linked to the presence of various flavonoids in Cd extract. Furthermore, in the current research, therapy of Cd extract caused substantial enhancements in CAT, GSH, SOD, MDA, NO, and H₂O₂. This extract's antioxidant activities can be described in part by the existence of glycosidic flavonoids, including quercetin, rutin, kaempferol, luteolin, isorhamnetin, and phenolic acids, which were previously found (Abdel Motaal et., al., 2011; Aparadh et., al., 2012).

The current data are consistent with those published (El-Naggar et., al. 2005), who revealed that Cd extract at rates of 100 and 200 mg/kg demonstrated considerable antiperoxidative action in alloxan rats with diabetes. Their results show a considerable increase in lipid peroxidation in rats that receive alloxan, which is reduced by Cd extract. Similarly, to the current results, (Fushiya et., al. 1999) identified, separated, and studied the inhibitory impact of two novel flavonoids from Cd extract on nitric oxide generation in macrophages that were stimulated in vitro. Additionally, (Cao et., al., 1998; El-(Shenawy & Abdel-Nabi, 2004; Nagy & Mohamed, 2015) showed that giving Cd extract resulted in an important rise in the amount of GSH in rats suffering from diabetes. That might suggest that the extract enhances GSH manufacturing and/or lowers oxidative stress, resulting in less GSH breakdown. likewise, levels of MDA were considerably lower in diabetic rats than in healthy control rats.

The raised overall antioxidant power of diabetic blood rats following Cd extract administration could be related to antioxidant uptake. Furthermore, treating rats with diabetes using Cd extract increased the rate of action of glucose-6-phosphate dehydrogenase (G6PDH). G6PDH serves a crucial part in glutathione production, based on the following research information: G6PDH regulates the proper amount of NADPH. Consequently, NADPH sustains GSH concentrations in hepatocytes, and GSH defends cells from ROS-induced oxidative harm. Cd extract induced an elevate in hepatic GSH concentration may improve the GSH/GSSG balance and reduce liver lipid peroxidation, hence improving physiological functioning (Mehta et., al., 2000). Evidence suggests that certain phytochemicals found in this extract, such as flavonoids, play a major role in treating or retarding a wide spectrum of diseases and are reported to possess anti-oxidative and anti-inflammatory properties (Al-Zail & Kamies., 2021)

CONCLUSION

The findings of this investigation showed that the *Cleome droserifolia* (Cd) extract has antioxidant protection effects against oxidative stress of cyhalothrin (Cy) of male albino rats.

ACKNOWLEDGEMENT

I would like to thank my institution, Omar Al-Mukhtar University, and the Faculty of Science, especially the Department of Zoology, for their moral support and for providing a suitable environment for study.

ETHICS

Authors should address any ethical issues that may arise after the publication of this manuscript.

Duality of interest: The authors declare no conflict of interest

Author contributions: Contribution is equal between authors.

Funding: The authors did not receive any funding (institutional, private, and/or corporate financial support)

REFERENCES

- Abdel Motaal, A., Ezzat, S.M. & Haddad, P.S. (2011). Determination of bioactive markers in *Cleome droserifolia* using cell-based bioassays for anti-diabetic activity and isolation of two novel active compounds. *Phytomedicine*, 19: 38-41.
- Abdul-Hamid, M., Mohamed, H. M., Abd El-Twab, S. M. & Zaied, K. (2020). Histological, ultra-structural, and biochemical study on the possible role of Panax ginseng in ameliorating liver injury induced by Lambda cyhalotherin. *BJBAS 9*(52): 1–18. https://doi.org/10.1186/s43088-020-00076-6
- Aebi, H. (1984). Catalase in vitro. *Methods Enzymol.*, (105):121–126.
- Al-Zail, N. I. and Kamies, S. F. (2021). A Study on the Effect of Samoa Extract (*Cleome droseriflia*) on Sperm Quality in Male Albino Rats Exposed to Pyrethroid. *Libyan Journal of Basic Sciences*, 5: 39-45. DOI:10.36811/ljbs.2021.110064
- Aparadh, V.T., Mahamuni, R.J. & Karadge, B.A. (2012). Taxonomy and physiological studies in spider flower (Cleome species): A Critical Review. *Plant Sciences Feed*, *2*(*3*): 25-46.
- Atamanalp, M., Kelep, M.S., Haluloulu, H.U. & Aras, M.S. (2002). The effects of cypermethrin (a synthetic pyrethroid) on some biochemical parameters (Ca, P, Na and TP) of rainbow trout (Oncorhynchus mykiss). *Turk J. Vet. Ani. Sci.*, 26: 1157-1160.
- Azab, A. (2025). Cleome Plants of Israel and Palestine: Smelly, Beautiful and Medicinally Active. A Review. *World Journal of Pharmaceutical Research*, *14*: (4): 01-37.
- Cao, G., Booth, S.L., Sadowski, J.A. & Prior, R.L. (1998). Increases in human plasma antioxidant capacity following consumption of controlled diets high in fruits and vegetables. *Am. J. Clin. Nutr.*, 68: 1081-1087.
- El-Askary, H.I. (2005). Terpenoids from *Cleome droserifolia* (Forssk.) *Del. Molecules.*, 10: 971-977.
- El-Demerdash, F.M. (2007). Lambda-cyhalothrin-induced changes in oxidative stress biomarkers in rabbit erythrocytes and alleviation effects of some antioxidants. *Toxicol. In vitro.*, 21: 392-397.
- El-Khawaga, O.A.Y., Abou-Seif, M.A., El-Waseef, A. & Negm, A.A. (2010). Hypoglycemic, hypolipidemic and antioxidant activities of *Cleome droserifolia* in streptozotocin-diabetic rats. *Journal of Stress Physiology & Biochemistry.*, 6 (4): 28-41.
- Ellman, G.L. (1959). Tissue sulfhydryl groups. Arch. Biochem. Biophys., 82(1):70–77.

- El-Naggar, E.M.B., Bartosikova, L., Zemlicka, M., Svajdlenka, E., Rabiskova, M., Strnadova, V. & Necas, J. (2005). Antidiabetic effect of *Cleome droserifolia* aerial parts: lipid peroxidation-induced oxidative stress in diabetic rats. *Acta. Vet. Brno.*, 74: 347-352.
- El-Shenawy, N.S. & Abdel-Nabi, I.M. (2004). Comparative analysis of the protective effect of melatonin and *Cleome droserifolia* extract on antioxidant status of diabetic rats. *The Egyptian Journal of Hospital Medicine.*, 14: 11-25.
- Ender, Y. & Onder, C. (2006). Effects of dichlorvos on lipid peroxidation in mice on subacute and subchronic periods. *Pest. Biochem. Physiol.*, 86: 106-109.
- Fetoui, H., Feki, A., Ben Salah, G., Kamoun, H., Fakhfakh, F. & Gdoura, R. (2013). Exposure to lambda-cyhalothrin, a synthetic pyrethroid, increases reactive oxygen species production and induces genotoxicity in rat peripheral blood. *Toxicol. Ind. Health, PMID.*, 23406951.
- Fetoui, H., Garoui, E.M. & Zeghal, E. (2009). Lambda-cyhalothrin-induced biochemical and histopathological changes in the liver of rats: ameliorative effect of ascorbic acid. *Exp. Toxicol. Pathol.*, *61*: 189-196.
- Fetoui, H., Garoui, M., Makni-Ayadi, F. & Zeghal, N. (2008). Oxidative stress induced by lambda-cyhalothrin (LTC) in rat erythrocytes and brain: attenuation by vitamin C. *Environ. Toxicol. Pharm.*, 26: 225-231.
- Fetoui, H., Makni, M., Garoui, M. & Zeghal, N. (2010). Toxic effects of lambda-cyhalothrin, a synthetic pyrethroid pesticide, on the rat kidney: involvement of oxidative stress and protective role of ascorbic acid. *Exp. Toxicol. Pathol.*, 62:593-599.
- Fushiya, S., Kishi, Y. & Hattori, K. (1999). Flavonoids from *Cleome droserifolia* suppress NO production in activated macrophages in vitro. *Planta Med.*, 65: 404-407.
- Green, L. C., Wagner, D. A., Glogowski, J., Skipper, P. L., Wishnok, J. S. & Tannenbaum, S. R. (1982). Analysis of nitrate, nitrite, and [15N] nitrate in biological fluids. *Anal. Biochem.*, 126 (1):131–138.
- Hoek, J. B. & Pastorino, J. G. (2002). Ethanol oxidative stress and cytokine induced liver damage. *Alcohol.*, 27: 63-68.
- Huang, T., Hsu, C., Chen, J., Liu, T. & Wei, H. (2003). Oxidative-stress related changes in the livers of bile-duct-ligated rats. *J. biomed. Sci.*, 10: 170-178.
- Kale, M., Rathore, N., John, S. & Bhatnagar, D. (1999). Lipid peroxidative damage on pyrethroid exposure and alterations in antioxidant status in rat erythrocyte: a possible involvement of reactive oxygen species. *Toxicol. Lett.*, 105: 197-205.
- Kumar, S.V., Christina, A.J.M., Geetha Rani, P.V., Nalini, G. & Chidambaranathan, N. (2009). Antifibrotic effect of *Cleome viscosa* Linn on Carbon tetra chloride (CCl4) induced liver fibrosis. *Der. Pharma. Chemica.*, 1(2): 92-96.

- Madbouly, M.S. (2003). Histological and histochemical studies on the effect of Atrazine (a herbicide) on the liver of albino rats and the prophylactic role of vitamin E. *Histology and Hitochemistry.*, 41: 63-76.
- Madkour, N.K. (2012). Protective effect of curcumin on oxidative stress and DNA fragmentation against lambda cyhalothrin-induced liver damage in rats. *Journal of Applied Pharmaceutical Science.*, 2(12): 76-81.
- Mehta, A., Mason, P.J. & Vulliamy, T.J. (2000). Glucose-6- phosphate dehydrogenase deficiency. *Baillieres Best. Res. Clin. Haematol.*, 13: 21-38.
- Nagy, M.A. and Mohamed, S.A. (2015). Cleome droserifolia (Cleomaceae) methanolic extract alleviates alloxan-induced oxidative stress and $\tilde{A}f\hat{A}\phi$ -cell damage in rat pancreas. BioChemistry: An Indian Journal, 9(1): (001-011).
- Nishikimi, M., Appaji, N. & Yagi, K. (1972). The occurrence of superoxide anion in the reaction of reduced phenazinemetho sulfate and molecular oxygen. Biochem. Biophys. *Res. Commun.*, 46(2):849–854.
- Ohkawa, H., Ohishi, N. & Yagi, K. (1979). Assay for lipid peroxides in animal tissues by thiobarbituric acid reaction. *Anal. Biochem.*, 95(2): 351–358.
- Prashanthi, N., Narayana, K., Nayanatara, A., Chandra Kumar, H.H., Bairy, K.L. & D'Souza, U.J. (2006). The reproductive toxicity of the organophosphate pesticide 0,0-dimethyl 0-4- nitrophenyl phosphorothioate (methyl parathion) in the male rat. *Folia. Morphol. (Warsz).*, 65: 309-321.
- Prior, R.L., Wu, X. & Schaich, K. (2005). Standardized methods for the determination of antioxidant capacity and phenolics in foods and dietary supplements. *J. Agric. Food Chem.*, *53*: 4290-4302.
- Rice Evans, C. (2004). Flavonoids and isoflavones: absorption, metabolism and bioactivity. *Free Rad. Biol. Med.*, *36*: 827-828.
- Rubilar, M., Pinelo, M., Ihl, M.; Scheuermann, E., Sineiro, J. & Nuñez, M.J. (2006). Murta leaves (Ugni molinae Turcz) as a source of antioxidant polyphenols. *Journal of Agricultural and food chemistry*, 54: 59-64.
- Sakr, S. and Rashad, W.A. (2023). Lambda-cyhalothrin-induced pancreatic toxicity in adult albino rats. *Scientifc Reports*, *18*(*13*): 11562. doi: 10.1038/s41598-023-38661-1
- Scherer, R. & Godoy, H.T. (2009). Antioxidant activity index (AAi) by the 2, 2-diphenyl-1- pic-rylhydrazyl method. *Food chemistry*, 112: 654-658.
- Tello, R. & Crewson, P.E. (2003). Hypothesis testing II: means. *Radiol.*, 227(1): 1-4.
- Velioglu, Y.S., Mazza, G., Gao, L. & Oomah, B.D. (1998). Antioxidant activity and total phenolics in selected fruits, vegetables, and grain products. *Journal of Agricultural food & chemistry*, 46: 4113-4117.

- Velmurugan, B., Selvanayagam, M., Cengiz, E.I. & Unlu, E. (2007). Histopathology of lambda cyhalothrin on tissues (gill, kidney, liver and intestine) of Cirrhinus mrigala. *Environ. Toxicol. Pharmacol.*, 24: 286-291.
- Wang, J. & Wang, H. (2017). Oxidative stress in pancreatic beta cell regeneration. *Oxid. Med. Cell. Longev.* https://doi.org/10.1155/2017/1930261
- Yadav, E., Kumar, V. and Sharma, H.N. (2023). Lambda cyhalothrin induced oxidative stress on brain tissues of rattus norvegicus and its amelioration by green tea extract. *International Journal of Biological Innovations*, 5(1): 103-108.